N.A.E.

R. & M. No. 2897
(14,771)
A.R.C. Technical Report

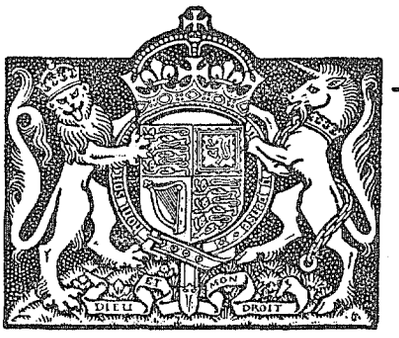

MINISTRY OF SUPPLY

AERONAUTICAL RESEARCH COUNCIL
REPORTS AND MEMORANDA

Boundary-layer Control for High Lift by Suction at the Leading-edge of a 40 deg Swept-back Wing

By

E. D. POPPLETON

LONDON: HER MAJESTY'S STATIONERY OFFICE
1955

TEN SHILLINGS NET

Boundary-layer Control for High Lift by Suction at the Leading edge of a 40 deg Swept-back Wing

By

E. D. POPPLETON

COMMUNICATED BY THE PRINCIPAL DIRECTOR OF SCIENTIFIC RESEARCH (AIR), MINISTRY OF SUPPLY

Reports and Memoranda No 2897*
October, 1951

Summary.—Wind-tunnel tests have been made on a 40 deg swept-back wing, 10 per cent thick with constant chord and an aspect ratio of 4·6. Boundary-layer control was applied along the whole leading edge, and a comparison was made between the effects of distributed suction and suction through a slot. A 45 per cent Fowler flap was used in some tests.

The overall effect of the two systems was similar, giving an increase in $C_{L\,max}$ by increasing the stalling incidence and making the wing statically stable up to the stall, when there was a severe loss of lift. At $R = 1{\cdot}29 \times 10^6$, a gain in $C_{L\,max}$ of 0·5 was obtained when $C_Q = 0{\cdot}0023$ with distributed suction over the first 2·5 per cent chord, while a C_Q of 0·0074 was needed to obtain the same increment with a slot (0·18 per cent chord wide at 2·5 per cent chord). A maximum value of $C_{L\,max}$ of 1·95 was obtained by both methods with flaps down at $\alpha = 25$ deg.

For full-scale application, the suction required for distributed suction (8·2 lb/sq in.) is much higher than for the slot, but it may be possible to reduce this by grading the porosity in a chordwise direction or by dividing the leading edge into a number of separate spanwise compartments. With the slot, the quantity required is higher but the overall power is about the same. A reduction in power may be possible in this case, by improving the shape of the slot.

As a means of producing high maximum lift on swept wings, both these methods have the disadvantage of requiring variable-incidence wings, if the full gain in $C_{L\,max}$ is to be used. Either method can be used as a means of preventing tip stalling as an alternative to nose flaps or leading-edge slots.

1. *Introduction.*—Two-dimensional tests on aerofoils having boundary-layer control by suction on the leading edge indicate that substantial gains in maximum lift coefficient may be achieved with fairly small suction quantities. The tests described in this report were designed to determine whether leading-edge suction would produce comparable increases in $C_{L\,max}$ on swept wings and, also, whether the tip stall could be prevented.

The model was originally constructed to have a porous leading edge extending from the wing-body junction to 89 per cent semi-span, this being replaced subsequently by a suction slot having the same spanwise extent. The tests on the wing with the porous leading edge have already been described in detail elsewhere by the present author[1] (1950), and only the more important results are presented here, together with those for the tests on the wing with the suction slot.

* R.A.E. Report Aero. 2440, received 2nd March, 1952. (Title of R. & M. changed from that of original Report to avoid confusion with other work.)

2. *Description of Model and Tests.*—2.1. *Description of Model.*—The tests were made on a half-model mounted on the lower balance in the No. 2, $11\frac{1}{2}$-ft Wind Tunnel at the Royal Aircraft Establishment. The aerofoil sections along wing were the HSA I profile ($t/c = 10$ per cent) the co-ordinates of which appear in Table 2. The aerofoil section was modified slightly near the nose to eliminate a slight shoulder which occurred on the original profile. This modification had the effect of reducing the leading-edge radius from 1·8 per cent chord to 1·4 per cent chord. The chord was constant except in the region of the tip where a curved leading edge (Küchemann tip) was fitted. The leading edge of the wing was swept back at 40 deg and the overall aspect ratio, assuming that the tunnel floor acted as a reflection plate, was 4·6. A fuselage was fitted and there was a gap of about 0·05 in. between the fuselage and the floor. A Fowler flap, extending from the body to 45 per cent semi-span, was fitted in some tests and the general arrangement of the model in this condition is shown in Fig. 1.

The porous leading edge extended spanwise from the body to the end of the parallel part of the wing and the maximum chordwise extent was from the leading edge to 11·2 per cent chord. The porous material used for covering the leading edge was end-grain beechwood. This material was chosen as it was thought that there was more hope of making an accurate contour with it than with either sintered bronze (Porosint) or rolled gauze. It also had a high resistance to flow, a pressure drop of 10 in. of mercury causing a normal velocity of 5 ft/sec through a thickness of $\frac{1}{8}$ in. A high resistance was thought desirable as the chordwise variation of pressure near the nose was expected to be large at high incidences.

The leading-edge covering was shaped from a plank in such a manner that the grain was at an angle of 20 deg to the chord-line, as shown in Fig. 2. By this means it was ensured that the inflow started at the leading edge and that the amount of porous area blanketed by the main structure was reasonably small. It was only possible to make the leading edge in small sections and it consisted of nine planks, with an average spanwise length of about 6 in. The loss in porosity at the glued joints, which were normal to the leading edge, only extended over a very small spanwise region.

The shape of the resulting nose was quite accurate, except for very slight flats which occurred at the leading edge due to the fact that it was impossible to use sandpaper for the final finish, as this would have clogged the pores. This accuracy was not maintained during the tests, however, as the end-grain wood was very susceptible to changes in moisture content. The drying due to increases in tunnel temperature during long runs, caused sufficient shrinkage for the joints between the planks to crack. Frequent repairs were necessary and these were carried out by filling the cracks with balsa and glueing, with a consequent loss of porosity. Any subsequent increase in moisture content caused an expansion of the planks and a bulging at the joints. Ultimately, it was decided to cover the joints between the planks with thin strips of Sellotape ($\frac{1}{16}$-in. wide) so that conditions were constant throughout the run, even if cracks appeared. This caused a complete loss of porosity at the joints.

The leading edge was divided into three independent sections of equal extent by plywood partitions (*see* Fig. 1) and the covering between the partitions was supported on 20 S.W.G. brass formers at 1-in. pitch (not shown in Fig. 1). Holes were drilled in these formers, so that all the compartments formed by them were interconnected, and the edges supporting the covering were bevelled in order to minimise their effect on the inflow distribution. Each of the three sections of the cavity under the beechwood was connected to a separate duct in the wing through a series of circular passages of $\frac{1}{2}$-in. diameter, each passage leaving the cavity between two of the brass formers.

After the tests on the model with the porous leading edge were completed, the beechwood covering was removed and replaced by an impermeable nose having a single suction slot extending from the root to the beginning of the curved tip. The mean width of the slot, normal to the leading edge, was 0·046 in. (0·18 per cent chord) and it was placed, parallel to the leading

edge, at a distance 2·5 per cent chord from it. No attempt was made to provide efficient diffusion from the slot throat, which opened directly into a relatively large cavity within the leading edge (Fig. 2). The plywood partitions, which divided the cavity under the porous leading edge into three compartments, were replaced by wooden formers of triangular plan form, the apex lying just downstream of the slot and the base fitting between two adjacent passages. Support for the leading edge was provided by a number of these formers which were evenly spaced, at about 6-in. pitch, in the three leading-edge compartments.

The three ducts in the wing tapered from an oval cross-section of major axis 2 in. and minor axis 0·7 in. at the outer end to a circle of 2 in. diameter at the wing root. From here the ducts were led into a junction box, where they joined a single outlet pipe, after passing through the metering orifice plates. In order that the model should be isolated from earth, the outlet pipe was joined to the main suction pipe through an air bearing. This consisted of two flat brass annular surfaces, one fixed to the outlet pipe of the junction box, and one fixed to the main suction pipe. The earthed surface had a ring of small holes drilled in it and was held in a contact with the annulus on the junction box by means of springs, the bearing surfaces so formed being lubricated by blowing compressed air through the small holes. This arrangement was very satisfactory and the effect of suction on the force measurements was negligible.

The flow through the three ducts was measured in the junction box by means of orifice plates. A series of orifices was available so that the ratio of the flows in the three ducts could be varied and the flow in any duct could be cut off by inserting a shutter in place of an orifice.

A line of pressure-plotting holes was fitted in the wing, along wind, at a station 67 per cent semi-span outboard of the centre-line of the body. The wing with the porous leading edge had thirty pressure holes while the slotted wing had two more fitted so that the pressures near the slot could be measured in more detail.

2.2. *Description of Tests.*—The distribution of flow into the porous leading edge was measured, with the wind off, by means of a venturi tube, having a cylindrical rubber pad at one end. This was pressed firmly on to the surface and it was thought that measurement of the static pressure in the throat gave a fair estimate of the average velocity through the area enclosed by the pad ($\frac{5}{16}$-in. inside diameter).

The spanwise distribution of slot velocity was measured by placing a reversed pitot in the slot throat. Tests had shown that the apparent velocity, obtained using the reading of the reversed pitot as the static pressure, was greater than the true velocity by a percentage that was roughly independent of speed. The velocity distribution could thus be determined with a fair degree of accuracy, by this means.

The ratio of flow through the three ducts was varied in some of the tests and the effect of variations in the area of the porous leading was edge investigated fully; three different chordwise extents were tested (2·5 per cent chord, 7·5 per cent chord, and 11·2 per cent chord), by covering part of the nose with Sellotape. Some tests were also made with the slot width increased to 0·11 in. (0·44 per cent chord), the increase being accomplished by paring away the downstream lip, so that the slot centre-line was moved slightly downstream in the process.

Measurements of lift, drag and pitching moment were made with several combinations of suction quantity and Reynolds number and the chordwise distribution of pressure, along wind, was measured at several incidences. These measurements were also made with the Fowler flap in position.

The tests were made at Reynolds numbers of 1·29, 2·24 and $2·58 \times 10^6$ and tunnel corrections for an unswept wing of the same area and aspect ratio have been applied to the results.

3. *Discussion of Results.*—3.1. *Flow Distribution (Wind Off).*—The spanwise distribution of flow into the porous leading edge, at three positions on the nose, is shown in Fig. 3, for the case where all the porous area (chordwise extent 11·2 per cent chord) was exposed. This distribution remained fairly constant as the suction quantity was varied and the mean velocity measured by the venturi agreed fairly well with that computed from measurements in the ducts. Due to the non-uniformity of the beechwood the normal velocity varied somewhat erratically from place to place. Moreover, as already mentioned, the joints in the leading edge were covered with strips of Sellotape during most of the tests. This non-uniformity does not appear to have had a very marked effect on the results but a uniform distribution would probably have reduced the quantities of air required by an appreciable amount.

The mean velocity through the outer section (Duct 3) was greater than that through the two inboard sections. The flow through Duct 3 was about $1\frac{1}{2}$ times that in the other two ducts and the difference may have been due to a higher porosity in the planks at the tip, as all three ducts were similar and were fitted with orifices of the same size. This distribution was used in most tests and, when the effect of changing the distribution was investigated, it was found that the one illustrated in Fig. 3 gave the largest increase in maximum lift coefficient.

The relation between the mean velocity through the leading edge and the total flow cofficient, C_Q, is of the form

$$\frac{v_m}{U_0} = nC_Q.$$

The values of n for the three extents of porous leading edge used in the tests are given in the following table :

Extent per cent chord	2·5	7·5	11·2
n	35	14	10

The distribution of velocity along the leading-edge slot is shown in Fig. 4. For this case the flow in the outboard duct (Duct 3) was about 50 per cent greater than that in the other two ducts. The variations in velocity along the span were less than in the case of the porous leading edge and the effect of variation of the mass flow on the velocity distribution was fairly small. The flow into the slot was very steady at all values of C_Q. With this distribution it was found that with small values of C_Q, the stall started at mid-span and spread slowly inboard and towards the tip as the incidence increased. In an attempt to delay the stall, the flow in Duct 2 was made equal to that in Duct 3, but the stall started at about the same incidence as before, although the first separation took place nearer the root. Most of the tests were made with this latter distribution but it was found that, at high values of C_Q, the maximum lift coefficient was insensitive to variations in flow distribution, within a fairly large range.

The mean slot velocity (corrected to Standard Temperature and Pressure) is given by

$$\frac{v_s}{U_0} = 530C_Q$$

for the slot of width 0·18 per cent chord.

3.2. *Lift, Drag and Pitching Moment.*—Some typical lift curves are shown in Figs. 5 and 6. The effect of both suction systems was to increase the slope of the curve (due to the decrease in boundary-layer thickness) and to increase the range wherein the curve is linear. In the case

of the wing without flap there was a change in the lift slope at a value of C_L of about 0·8, and this was accompanied by an increase in dC_M/dC_L. This was probably caused by a localised separation near the tip where there was no boundary-layer control. A similar change in slope occurred with the flap in position, but here the effect was not so marked. With suction, the character of the stall changed fairly rapidly from the gradual type encountered with no suction to the sharp drop in lift shown for the higher values of C_Q. With the porous leading edge, the transition to the very abrupt stall occurred more gradually as the extent of the porous leading edge was increased.

It was found that there was a considerable hysteresis effect present with both suction systems and, when the wing had stalled, a fairly large decrease in incidence was required to re-establish unseparated flow. When the stall took place at $\alpha = 27$ deg, for example, a reduction of 8 deg in incidence was required before the flow re-attached. Alternatively, the wing could be unstalled by increasing the suction, at constant incidence. At $\alpha = 20$ deg, the increase in suction quantity required was found to be of the order of 100 per cent.

The results of the tests on the wing with porous leading edge without suction, the leading-edge slot with $C_Q = 0$ (the ducts at the wing root were blanked off to achieve this), and with the leading-edge slot filled in with Plasticine, were all in reasonable agreement. There was some scale effect difference, but the pitching-moment curves (Fig. 7) show that the wing without suction became statically unstable at $C_L = 0{\cdot}6$ without the flap and at $C_L = 1{\cdot}1$ with the flap fitted ($R = 1{\cdot}29 \times 10^6$). Fig. 7 shows that the effect of suction was to make the wing stable up to the stall and to increase the slope of the C_M vs. C_L curve slightly. At the stall, the change in trim on the slotted wing was much larger than that on the wing with the porous nose, the decrease in $-C_M$ on the unflapped wing being associated with a drop in lift considerably greater than that encountered with distributed suction.

The minimum value of C_D/C_L was not altered greatly by suction (Fig. 8), but the range wherein the ratio was near the minimum was extended. In fact, the profile drag remained sensibly constant until the wing stalled, as will be seen from Fig. 9, where the drag coefficient is plotted against C_L^2. The drag recorded by the tunnel balance included that due to the destruction of the momentum of the air absorbed, as this was discharged vertically downwards through the tunnel floor. The increment in drag coefficient due to suction amounts to $2C_Q$ and this has been subtracted from the balance readings to obtain the values shown in Figs. 8 and 9. The curves thus correspond to the case of an aircraft where the controlling air is ejected downstream at free-stream velocity.

3.3. *Maximum Lift Coefficient.*—The increase in maximum lift coefficient due to suction is shown plotted against total quantity coefficient in Fig. 10. As has been mentioned already, the stall, at small values of C_Q, was very gradual and it was difficult to determine the value of of $C_{L\max}$ very precisely due to the unsteady conditions prevailing. For this reason, values of $C_{L\max}$ less than the no-suction value were sometimes recorded and the shape of the curves near the origin was thus rather ill-defined.

The effect of the two methods of control was roughly similar in that there was a range of C_Q in which suction caused only a small increase in $C_{L\max}$ and in which the flow conditions were unsteady. This was followed by an abrupt rise in $\Delta C_{L\max}$, wherein most of the gain in maximum lift took place, after which the curves flattened and presumably approached a maximum increment asymptotically. In the case of the wing with the porous nose, some values of $C_{L\max}$ greater than those shown in Fig. 10 were obtained before the cracks appeared in the leading edge. This deterioration in shape near the leading edge caused a loss of about 17 per cent in the value of the maximum increment in $C_{L\max}$.

The quantity required to attain a given $C_{L\max}$ with distributed suction was much less than that required with the suction slot, the quantity for the 2·5 per cent porous leading edge being about one third that required for the slot of width 0·18 per cent chord. The curves also show that, with distributed suction, there was an increase in economy if the extent of the porous surface was decreased. A similar effect was produced by reducing the slot width and qualitative explanation of these phenomena is given in section 3.4 where the chordwise distribution of pressure is discussed.

There was a considerable scale effect on the C_Q required to maintain a given $C_{L\max}$ with both suction systems, the effect being greater in the case of the slotted wing. The nature of the scale effect seemed to differ in the two systems for, whereas the curves for the slot lie parallel in the region of rapid rise in $\Delta C_{L\max}$, the two curves converge in the case of the porous nose. The curve for the higher Reynolds number has the smaller slope and it appears that, at higher values of C_Q, the C_Q required to attain a given $C_{L\max}$ would be greater than at the lower Reynolds number. Whether, in fact, the two curves do intersect could not be determined as the attainment of higher quantity coefficients at $R = 2{\cdot}58 \times 10^6$ would have led to dangerously high pressure drops with possible large distortion and damage to the leading edge. A possible reason for these differing scale effects is given in section 5.

The drag coefficient equivalent of the power required to suck away the boundary layer and eject it downstream at free-stream total head is given by

$$C_{Dp} = (1 + C_s)C_q$$

where $C_s = (p_0 - p_s)/\frac{1}{2}\rho_0 U_0^2$

p_s is the static pressure in leading-edge cavity.

This assumes that the velocity in the cavity is zero, that the subsequent ducting is frictionless and that the efficiency of the pump is the same as the propulsive efficiency of the aircraft power plant.

The increments in $C_{L\max}$ are shown plotted against C_{Dp} in Figs. 11 and 12, for the case with the 2·5 per cent chord porous nose and for the case with the 0·18 per cent chord slot. The power required to maintain a given $C_{L\max}$ was found to be roughly independent of the chordwise extent of the porous nose so that the 2·5 per cent chord extent is probably the most convenient for practical application as the quantity required is less than for the larger extents. The curves show that the suction slot required less power to maintain the higher values of $\Delta C_{L\max}$ at both Reynolds numbers.

Also included on Fig. 12 is a curve showing the variation $\Delta C_{L\max}$ with power for the case where the slot was widened to 0·0044c. The narrower slot appears to require less power over most of the range.

3.4. *Pressure Distribution.*—Typical pressure distributions are shown in Figs. 13, 14 and 15, where the distributions for the wing with the 0·18 per cent chord leading-edge slot are compared with those for the porous leading-edge case. A feature of all the high-incidence curves is the very large peak suction near the leading edge with the steep adverse gradient following it. Due to the ' sink effect ' of the slot, the velocities over the nose were increased considerably above those present in the case of the porous leading edge, which may be taken to represent fairly closely potential flow conditions in that region. In one test on the wing with the leading-edge slot a local Mach number of 0·77 was recorded at a lift coefficient of 1·62, when the tunnel Mach number was 0·18.

The pressure distribution over the rear of the aerofoil with the porous leading edge differed from that with the slot. This may be due to the fact that the boundary layer leaves the porous leading edge with a finite thickness whereas it starts on the downstream lip of the slot with virtually zero thickness. In the case of the 2·5 per cent chord porous leading edge, it then has to flow against quite a large adverse gradient with the result that when the rear of the aerofoil is reached, the boundary layer is much thicker than that on the slotted wing. This results in a less complete pressure recovery. This conclusion is confirmed by the fact that the disturbance to the distribution illustrated in Fig. 14 is much less marked, and here the porous leading edge extended over 11·2 per cent chord thus covering the steep part of the adverse gradient so that the growth of the boundary layer was retarded.

The pressure distribution on the upper surface after the stall is also shown on Fig. 14. As has been remarked the onset of the stall was extremely rapid at high values of C_Q and only a very small increase in incidence was necessary to cause a complete collapse of the suction peak on the leading edge. The flow near the stall was very unstable and frequently separation occurred while readings of the pressure distribution were being made, and conditions in the tunnel were apparently constant.

The distribution for the porous leading edge shown in Fig. 14 was used as a rough guide for determining the position of the leading-edge slot. It was decided to locate it about half-way along the steep adverse gradient as rough calculations of the sink effect produced by a slot with a reasonable value of C_Q, indicated that the gradient would then be split into two smaller ones, neither of which would be large enough to cause separation.

The pressure distributions for the aerofoil with the porous leading edge indicate a possible explanation for the increase in economy accompanying a decrease in the extent of the porous nose. It will be seen from Figs. 13 and 14 that the majority of the pressure rise is confined to the first two or three per cent of the chord. It is not unreasonable therefore, that suction concentrated in this region should be more effective than if spread over a larger area, but it is probable that the smallest extent used in the tests ($2\frac{1}{2}$ per cent chord) is near the optimum value. Any further decrease would probably lead to a deterioration in the performance of the wing, since the ensuing uncontrolled adverse gradient might become large enough to cause separation.

Fig. 16 shows the pressure distribution ahead of the slot at an incidence just below the stall with a slot width of 0·18 per cent chord. The value of C_p in the slot throat has been estimated and this indicates that there is a favourable pressure gradient into the slot. If the slot width is increased to 0·44 per cent chord, keeping C_Q and α constant, the value of $-C_p$ in the throat decreases and an adverse gradient appears which causes the flow to break down. In order to re-establish the flow it is necessary to increase C_Q until the adverse gradient is eliminated, the measured pressure distribution for this case being included in Fig. 16. This suggests that the slot width should be kept small, approaching as closely as possible the ideal sink, where the inflow velocity is infinite. In practice, the slot must be made sufficiently large to avoid choking at the required value of C_Q.

Figs. 17 and 18 show details of the pressure distribution near the nose of the slotted wing, for several values of C_Q, compared with the distribution over the porous leading edge.

The pressure distributions for the wing with the porous leading edge were integrated to give the local resultant force and this was converted to a local lift coefficient. This lift coefficient is shown plotted against incidence in Fig. 19, together with the total lift coefficient, obtained from balance measurements.

4. *Comparison with Previous Experimental Results.*—Previous experimental work on the application of leading-edge suction to swept wings has shown rather disappointing results. Details of the models used in two series of tests are given in the following table.

	Slot width $= 0{\cdot}01c$	$10\%c$ porous leading edge
Aspect ratio	4·5	5·09
Taper ratio	4 : 1	.3·23 : 1
Sweep of quarter-chord line	45°	40°
Spanwise extent of front slot or porous leading edge	$59\%s$ to $98\%s$	$40\%s$ to $100\%s$
Spanwise extent of rear slot	$38\%s$ to $60\%s$	—
Chordwise position of front slot	$6\%c$	—
Chordwise position of rear slot	$24\%c$	—
Reynolds number	$0{\cdot}83\times10^6$	$0{\cdot}80\times10^6$
$C_{L\max}$ without suction	1·03	1·02

The values of $\Delta C_{L\max}$ obtained in these tests are reproduced in Fig. 20 together with the lower Reynolds number results for the present model and it is seen that considerably higher lift increments have been obtained in the tests described herein. Some measurements were made on the present model with the inboard end of the slot filled in with Plasticine, so that the slot extended effectively from 30 per cent semi-span to 89 per cent semi-span. The results are similar to those obtained on the other two models (Fig. 20), the abrupt rise in $\Delta C_{L\max}$ characteristic of the full-span slot being absent. The nature of the stall, in this condition, was similar to the no-suction case, the value of the lift fluctuating erratically so that a precise measurement of $C_{L\max}$ was not possible. Tufts showed that the stall started at the inboard end of the slot, became fully established there, and then spread outboard along the trailing edge, until only a small area behind the slot remained unstalled.

Although these two series of tests are not strictly comparable with those described in this report since the wings were tapered and the Reynolds numbers and aspect ratios were different, it is significant that, in both cases, the boundary-layer control was limited to the outboard part of the wing only. This does seem to indicate that, if full benefit is to be derived from the leading-edge suction, it must be applied along the whole span.

5. *Scale Effect.*—5.1. *Scale Effect for Porous Leading Edge.*—With the small values of C_Q that were used, distributed suction has a negligible effect upon the potential flow velocity distribution. Control is therefore exercised on the boundary layer directly, by so retarding its growth that it leaves the porous surface with sufficient energy to reach the trailing edge without separating. At a given incidence, therefore, the velocity distribution outside the boundary layer is independent of Reynolds number and C_Q, and, if the flow over the nose is laminar and conditions of dynamic similarity prevail, then a given value of $C_{L\max}$ will occur at a constant value of $C_QR^{1/2}$. The flow over the solid part of the nose was almost certainly laminar as the boundary layer in this region would be very thin and in addition, it was flowing in a steep negative pressure gradient. It would thus be very stable, and its stability would increase on reaching the porous surface.

The values of $C_{L\max}$ obtained from Fig. 10 are replotted in Fig. 21 with $C_QR^{1/2}$ as abscissa. It will be seen that in each case, the results for the different Reynolds numbers lie on two distinct curves and, whereas a smaller value of $C_QR^{1/2}$ is required to maintain small values of $C_{L\max}$ at the larger Reynolds number, for higher values of $C_{L\max}$ the low Reynolds number case requires the smaller $C_QR^{1/2}$.

Probably the main reason for the discrepancy between the curves at low values of C_Q is that, as the incidence is increased, without suction, a condition is reached where the adverse gradient

on the nose is sufficient to cause a laminar separation and re-attachment. Suction has very little effect on the wing-stalling characteristics until this region of separated flow is removed. There is thus a minimum useful value of C_Q, which decreases with increasing Reynolds number since the extent of the laminar separation diminishes as the Reynolds number is increased. After the minimum C_Q has been exceeded the flow over the nose is entirely laminar so that it would be reasonable to suppose that the curves for the two Reynolds numbers would approach one another and join a common curve at large values of C_Q. In fact, the experimental curves appear to cross over so that it is probable that conditions of dynamic similarity were not fulfilled in the flow over the nose.

Dynamic similarity implies similarity of the distributions of inflow into the leading edge. This distribution has been calculated for an experimental pressure distribution using the method given in Appendix I and is presented in Fig. 22. The inflow distribution for the same incidence has also been calculated for a Reynolds number of $1 \cdot 29 \times 10^6$, assuming that C_Q varies inversely as $R^{1/2}$ and the porosity remains unchanged. The distributions differ considerably and, although both have a region of low velocity near the nose, where the external pressure is low, the variations of inflow, along the surface, are much larger in the case of the higher Reynolds number. Dynamic similarity cannot exist in the two flows over the nose, therefore, and an increase in Reynolds number at constant incidence causes a deterioration in the inflow distribution. The suction becomes weaker near the nose, where the majority of the pressure rise takes place, so that, if the suction quantity is varied according to the low $C_Q R^{1/2} = \text{constant}$, the maximum lift coefficient will fall as the Reynolds number increases. This effect would not have been so great had the leading edge been divided into a number of separate compartments, each having its own source of suction, and having the divisions so arranged that the variation of pressure, along the surface controlled by each compartment, was small. The change in velocity distribution may be eliminated entirely by changing the porosity distribution of the leading edge as the Reynolds number is varied in the manner indicated in Appendix II.

The distribution of inflow for the case where the porous area has been reduced to $2 \cdot 5$ per cent chord is also illustrated in Fig. 22. The change in distribution due to doubling the Reynolds number is not so large as when all the porous area is operative, so that it is possible that the scale effect on the quantity required for a given $C_{L\,\max}$ will not be so great, in this case. The test results for the $2 \cdot 5$ per cent chord porous leading edge are shown on Fig. 21 but the range of C_Q covered at the higher Reynolds number is not sufficient to verify this conclusion.

The results of the present tests may only be extrapolated to full-scale if it is assumed that the porosity of the leading edge is changed in a manner which will maintain a constant inflow distribution. Provided the value of $C_{L\max}$ required at full-scale is sufficiently large, the value of C_Q may then be assumed to vary inversely as $R^{1/2}$.

The condition for similarity of inflow distributions is shown in Appendix II to be

$$KR^{3/2}(C_p + C_s) = \text{constant}$$

where K is the porosity of the leading edge. Since the values of C_s required to maintain high maximum lift coefficients in the tests at $R = 1 \cdot 29 \times 10^6$ were very large, it is unlikely that values greater than these could be tolerated, at full scale, as very low pressures in the suction chamber would result. The value of C_s to be used in a practical full-scale design may therefore be assumed to lie between that used in the test, in which case the porosity is distributed along the chord as in the test, and local value of $-C_p$. In this latter ideal case, the leading-edge cavity is assumed to be divided into an infinity of separate compartments, the resistance of the surface being everywhere zero. The values of C_{Dp} calculated from these values of C_s will then form the upper and lower limits within which the pump drag will fall in practice. The lower value represents the power required to restore the energy deficit in that part of the boundary layer which is sucked away, since all other losses have been eliminated.

5.2. *Scale Effect for Suction Slot.*—The mechanism whereby the boundary layer is controlled by the slot is more complex than that in the case of the porous leading edge. Control is effected indirectly by so modifying the external pressure distribution, under the action of the sink effect of the slot that separation is delayed until the slot throat is reached. The process is further complicated by the fact that, even at small forward velocities, the flow over the surface near the slot may be approaching sonic conditions.

Although the suction quantities involved in this method of control are relatively large, rough calculations indicate that, at high incidences, the quantity absorbed by the slot may not have been much greater than that flowing in the boundary layer. In these calculations, it was assumed that the flow was incompressible and laminar and that conditions were the same as on an infinite yawed wing. It was found that the boundary-layer thickness at the pressure-plotting hole, just upstream of the slot ($s/c = 0{\cdot}031$) was about one-third of the slot width of $R = 1{\cdot}29 \times 10^6$ and $\alpha = 25{\cdot}9$ deg. The pressure distribution for this case is shown in Fig. 13.

When the Reynolds number is increased by increasing the forward speed, compressibility has some effect on the pressure distribution near the slot. If, however, as a first approximation, this effect is ignored and it is assumed that it is necessary to suck away a constant proportion of the boundary layer to maintain a given $C_{L\,\max}$ at all Reynolds numbers, then the scale effect on C_Q can be calculated. For a laminar layer, this assumption leads to the usual $C_Q R^{1/2}$ law, and, if the flat-plate relationship for the boundary-layer thickness is assumed to hold in a pressure gradient then C_Q varies inversely as $R^{1/5}$ for a turbulent boundary layer.

The laminar law appears to fit the no-flap results fairly well (Fig. 23). Those for the wing with flap, however, fall about midway between the values given by the formulae for the laminar and the turbulent boundary layers, and it was found that the relationship $C_Q R^{0{\cdot}31} = \text{constant}$ was more consistent with those results. This difference may be due to the effects of compressibility since the supervelocities on the nose of the wing with flap were greater than those on the plain wing. It may also be partly due to transition having taken place upstream of the slot. This is more likely to occur on the wing with flap since, at the larger values of $C_{L\,\max}$ attained, the stagnation point is farther downstream on the lower surface, and the boundary layer travels farther before reaching the slot.

The scale effect on C_{Dp} is not readily predictable. In Appendix III it is shown that the pump drag may be written

$$C_{Dp} = \left(\frac{C_Q}{F}\right)^3 \cdot \frac{\rho_s}{\rho_0} \cdot \frac{l_w}{S} \cdot \left[2\,\frac{\vartheta_s}{w} + f\,\frac{w'}{w}\right].$$

The variation of F, f and ϑ_s with C_Q and R is unknown but a rough estimate of C_{Dp} may be made by assuming that the coefficient of $C_Q{}^3$ remains constant. This is probably a pessimistic assumption if the Reynolds number is varied by increasing the linear dimensions, since in this case, f and ϑ_s/w will probably decrease and F increase. An increase in Reynolds number involving an increase in speed, however, may make extrapolations optimistic since F decreases as the mass flow per unit area of slot increases. The fall in F becomes quite rapid as choking conditions are approached.

This method of allowing for scale effect was applied to the test results but it was only successful in the case of the wing with flap. In this case if it was assumed that C_Q obeyed the 1/5 power law and, hence that C_{Dp} varied inversely at $R^{3/5}$ the experimental points lay fairly close to a common curve (Fig. 24). This suggests that the scale effect, which caused C_Q to diverge from the 1/5 power law in this case, is counterbalanced by the variation of $C_{Dp} C_Q{}^{-3}$ with Reynolds number.

6. *Application to Full-Scale Aircraft.*—The results of the preceding section may be used to form an estimate of the relative merits of the two systems of control, when applied to a full-scale aircraft.

Taking a typical single-engine swept-wing fighter the following results are obtained:

TABLE

Wing area	350 sq ft
Wing loading	45 lb/sq ft
$C_{L\max}$	1·9
Wing incidence at stall	25 deg
Stalling speed (V_s)	85 knots
Approach speed ($1{\cdot}3V_s$)	110 knots

		11·2%c porous leading edge	0·18%c slot
Q cu ft/sec (at stall)		80	250
Suction required (at stall) lb/sq in. below atmospheric pressure	Max	8·2	0·8
	Min	2·2	0·4
Power (at stall) h.p.	Max	170*	60
	Min	45	30

* Correction to figure in Ref. 1.

Two values of the estimated quantities are listed above and, for the porous leading edge, the maximum values correspond to the use of the test value of C_s. This ensures an inflow distribution similar to that in the test if the porosity is scaled from the test value inversely as $R^{3/2}$. The minimum values are for a more practical case than that mentioned in section 5.1. Here, a single leading-edge compartment is assumed and the porosity is so graded along the chord that, for the same inflow distribution that obtained in the test, the value of C_s is equal to the maximum value of $-C_p$ occurring on the nose. The resistance of the surface is thus zero at the peak suction point. This minimum value of the power could be further reduced by dividing the leading edge into a number of separate compartments and so approximating to the ideal conditions mentioned in section 5.1. It has been shown by Pankhurst and Gregory[3] (1948) that, on a two-dimensional wing, it is possible to halve the power required, by increasing the number of compartments from one to three. Moreover, a finer adjustment to the distribution of inflow is possible if there are several compartments and it is probable that such an arrangement would lead to a reduction in quantity, due to the more effective application of the suction. This would have the effect of further reducing the power required.

The 11·2 per cent chordwise extent of porous nose was used in this example as it was the only one on which a $C_{L\max}$ of 1·9 was achieved in the test. The quantity would probably be reduced by decreasing the extent of the porous area but it is obvious that further development work is needed before the most economical configuration can be determined.

For the case of the suction slot the quantity has been determined on the assumption that C_Q follows the 1/5 power rule, so that this value may err on the large side (*see* section 5.2).

The maximum value of the power quoted in the table is obtained using a pump drag coefficient scaled from the test result according to the relation $C_{Dp}\,R^{3/5} = \text{constant}$. As was explained in section 5.2, this probably gives a pessimistic estimate as the increase in Reynolds number is due to an increase in linear dimensions. Moreover, the estimate assumes that the slot remains

geometrically similar and, since the slot used in the tests was very inefficient it is probable that the value of C_{Dp} would be further reduced if an efficient diffuser were fitted. It is shown in Appendix III that

$$C_{Dp} = \left(\frac{C_Q}{F}\right)^3 \frac{\rho_s}{\rho_0} \frac{lw}{S} \left[2 \frac{\vartheta_s}{w} + f \frac{w'}{w} \right] .$$

where f is the proportion of the dynamic head at the throat that is lost in diffusion. The value of f was found to vary between $1 \cdot 1$ and $0 \cdot 8$ in the tests and, since ϑ/w is unlikely to be much greater than $0 \cdot 2$, even if the boundary layer fills the slot, it is possible that the fitting of an efficient diffuser might reduce the value of C_{Dp} by as much as a half. A minimum value of the power of one-half the maximum has, therefore, been quoted in the table, although it may well be possible to reduce this value still further by careful design.

An estimate of the suction required has also been obtained for the two values of power quoted, from the relation $C_{Dp} = (1 + C_s)C_Q$ and these are included in the table.

Comparison of the full-scale performance of the two methods of control reveals that, although the slot requires about three times the quantity used by the porous leading edge, the power required for a practical arrangement would be of the same order. It is also apparent that, with careful design, this power can be reduced to quite a low value. The suction required by the porous leading edge appears to be considerably greater than that required by the slot, the minimum value quoted being irreducible since it corresponds to the value of the minimum pressure on the nose.

7. *Conclusions.*—The present tests indicate that considerable gains in maximum lift coefficient may be achieved by the use of boundary-layer control by suction on the leading edge of a swept-back wing, in conjunction with a Fowler flap. Control by distributed suction and by slot had precisely the same overall effect, the linear part of the lift curve being extended and the wing remaining stable up to the stall, both with and without flap. The quantity required to maintain a given $C_{L\max}$ with slot suction was about three times that required by the porous leading edge but it was estimated that the power required by the two systems, in a practical application, would be about the same. It was not possible to decide which of the two systems would be the most convenient, in practice, as this would depend largely on such practical consideration as ease of manufacture and maintenance, the effect of leading-edge contamination on the economy of the system and the method of supplying the power. Both systems suffer from the disadvantage that, as the increased lift results from an extension of the lift curve, the stalling incidence is large.

The quantity required by the porous leading edge to maintain a given $C_{L\max}$ was found to decrease as the porous area was reduced, a reduction in chordwise extent from $11 \cdot 2$ per cent chord to $2 \cdot 5$ per cent chord resulting in a 30 per cent fall in C_Q. It was thought, however, that this was about an optimum value, as the majority of the pressure rise occurred within the first 3 per cent of the chord and any further reduction in porous area would probably have led to loss in boundary-layer control. The power required to achieve a given $\Delta C_{L\max}$ was roughly independent of the area of the porous leading edge. The performance of the wing was shown to be dependent on the porosity of the leading edge and the lift increments measured at low Reynolds numbers would not be attained economically at a larger scale unless the porosity of the leading edge were modified. This could be achieved by grading the porosity in a chordwise direction, or by dividing the leading edge into a number of spanwise compartments and so arranging the suction in these compartments that the inflow distribution is similar to that which obtained in the tests. It is quite possible that the porosity distribution used in the tests was not the optimum and that a more economical system would have resulted had the inflow been so arranged that it was concentrated between about 1 per cent chord and 4 per cent chord where the adverse gradient was steepest.

The economy of the slotted wing was found to depend critically on the slot width and it was thought that the nearer the slot approached the ideal sink, the smaller the quantity that would be required for a given $C_{L\max}$. In practice, the size of slot is limited by choking conditions, and the best full-scale design would probably be one in which the slot is just not choking when the required $C_{L\max}$ is attained.

The best spanwise distribution of flow into the porous leading edge was that in which the flow near the tip was about 50 per cent greater than that near the root, but the performance of the slotted wing was independent of spanwise flow distribution. It was found that, with both methods of control, the stalling characteristics deteriorated if the suction was confined to the outer part of the wing. This is in accordance with previous work on the subject and it was concluded that it is necessary to apply boundary-layer control along the whole leading edge, if full benefit is to be derived from it.

8. *Acknowledgment.*—The author wishes to acknowledge the assistance in the computational and experimental work given by Miss M. B. Whittaker.

REFERENCES

No.	*Author*	*Title, etc.*
1	E. D. Poppleton	Wind-tunnel tests on a swept-back wing having distributed suction on the leading edge. R.A.E. Tech. Note Aero. 2081. A.R.C. 13,796. November, 1950. (Unpublished.)
2	G. F. Moss	Low-speed wind-tunnel tests with suction slots on a wing with 45-deg sweepback. R.A.E. Tech. Note Aero. 1893. A.R.C. 10,692. May, 1947. (Unpublished.)
3	R. C. Pankhurst and N. Gregory ..	Power requirements for distributed suction for increasing maximum lift. C.P. 82. September, 1948.

LIST OF SYMBOLS

α Wing incidence (along wind)

b Wing span

c Local wing chord (along wind)

$\bar{c}$ Mean chord (along wind) $= S/b$

C_q Local quantity coefficient

$= \int \frac{\rho v}{\rho_0 U_0} d\left(\frac{s}{c}\right)$ for distributed suction

$= \frac{\rho_s v_s w'}{\rho_0 U_0 c} \sec \phi$ for slot

C_Q Total quantity coefficient $= \frac{Q}{U_0 S} = \int \frac{c}{S} \cdot C_q \, dy$

C_D	Measured aerodynamic drag coefficient = Drag/$\frac{1}{2}\rho_0 U_0^2 S$
C_{Dp}	Drag coefficient equivalent of pump power = $(1 + C_s)C_Q$
C_L	Lift coefficient = Lift/$\frac{1}{2}\rho_0 U_0^2 S$
C_M	Coefficient of the moment about the assumed c.g. position = (Pitching moment)/$\frac{1}{2}\rho_0 U_0^2 S\bar{c}$
C_s	Suction coefficient = $(p_0 - p_s)/\frac{1}{2}\rho_0 U_0^2$
C_p	Pressure coefficient = $(p - p_0)/\frac{1}{2}\rho_0 U_0^2$
δ	Boundary-layer thickness
δ_s^*	Displacement thickness of boundary layer at slot throat $= \int_0^\delta \left(1 - \frac{u}{v_s}\right) dy$
f	Proportion of $\frac{1}{2}\rho_s v_s^2$ lost in diffusion from slot throat
F	$C_Q U_0/v_s$
ϕ	Sweepback angle
K	Leading-edge porosity such that $v/U_0 = KR(C_p + C_s)$
l	Length of slot (parallel to leading edge)
p	Static pressure on aerofoil surface
p_0	Free-stream static pressure
p_s	Static pressure in leading-edge cavity
Q	Total quantity flowing through leading edge at S.T.P.
R	Reynolds number = $U_0\bar{c}/\nu$
ρ	Density at aerofoil surface
ρ_0	Density in free stream
ρ_s	Density in slot throat
s	Distance along aerofoil surface from leading edge
S	Wing area
ϑ_s	Energy thickness of boundary layer at slot throat $= \frac{1}{2}\int_0^\delta \left[1 - \left(\frac{u}{v_s}\right)^2\right]\frac{u}{v_s} dy$
u	Velocity in boundary layer at distance y from surface
U_0	Free-stream velocity
v	Velocity of flow into porous leading edge
v_m	Mean velocity of flow into porous leading edge
v_s	Slot velocity
w	Slot width (normal to leading edge)
w'	Effective slot width = $w - \delta_s^*$
x	Distance measured along chord-line from leading edge
y	Distance along wing normal to body centre-line and distance from surface in boundary layer

APPENDIX I

The Calculation of the Inflow Distribution on the Porous Leading Edge

Tests on specimens of end grain beech showed that, for small flows, the velocity through the surface was directly proportional to the pressure drop. It is reasonable to assume, therefore, that conditions were laminar and, by analogy with pipe flow, that the local flow into the leading edge could be expressed in the form

$$v = \frac{2kd^2}{\mu t}(p - p_s)$$

where k is a constant
d is the diameter of the pores
t is the thickness of the porous covering
p is the external static pressure
p_s is the static pressure in the leading-edge cavity.

This may be written

$$v = \frac{2kd^2}{\mu t} \cdot \tfrac{1}{2}\rho_0 U_0^2 (C_p + C_s)$$

or

$$\frac{v}{U_0} = KR(C_p + C_s) \qquad \ldots\ldots\ldots\ldots\ldots\ldots\ldots\ldots \quad (1)$$

where $K = \dfrac{kd^2}{t\bar{c}}$, the leading-edge ' porosity '

$R = U_0\bar{c}/\nu$
$C_p = (p - p_0)/\tfrac{1}{2}\rho_0 U_0^2$
$C_s = (p_0 - p_s)/\tfrac{1}{2}\rho_0 U_0^2$
$U_0 =$ free-stream velocity
$p_0 =$ free-stream static pressure.

The local quantity coefficient is then given by

$$C_q = \int \frac{\rho v}{\rho_0 U_0} d\left(\frac{s}{c}\right) = \int \frac{\rho}{\rho_0} KR(C_p + C_s)\, d\left(\frac{s}{c}\right) \qquad \ldots\ldots \quad (2)$$

and the total quantity coefficient is

$$C_Q = \int \frac{2c}{\bar{c}} \int \frac{\rho v}{\rho_0 U_0} d\left(\frac{s}{c}\right) d\left(\frac{y}{b}\right). \qquad \ldots\ldots\ldots\ldots \quad (3)$$

Equation (1) was used to calculate the inflow distributions illustrated in Fig. 22.

APPENDIX II

Conditions for Dynamic Similarity of Flow over the Porous Leading Edge

The conditions for dynamic similarity in the flow of laminar boundary layer over the porous noses are :

(*a*) The external pressure distribution must be constant
(*b*) The inflow distribution must be constant
(*c*) $C_q R^{1/2} =$ constant.

APPENDIX II—*continued*

The first condition is satisfied if the incidence of the aerofoil is unaltered. The second implies that at a given point on the surface the value of v/v_m must always be the same which, using the third condition and equation (1) leads to

$$KR^{3/2}(C_p + C_s) = \text{constant.} \quad \ldots \quad \ldots \quad \ldots \quad \ldots \quad \ldots \quad \ldots \quad \ldots \quad (4)$$

Hence, with laminar flow, if a certain $C_{L\max}$ is achieved at a given Reynolds number and a given value of C_q, then the same value of $C_{L\max}$ will be attained at another Reynolds number only if the local porosity of the leading edge is varied according to equation (4) and the quantity coefficient satisfies the relation $C_qR^{1/2} = \text{constant}$.

The above argument is valid only if the stall is due to laminar separation from the leading edge at all the Reynolds numbers considered.

APPENDIX III

The Evaluation of C_{Dp} for the Slotted Wing

The pump has to make good the energy deficiency in the boundary layer and the loss in total head due to diffusion. If it is assumed that conditions do not vary along the span, then the total energy lost per second in the boundary layer at the slot throat is given by

$$l\int_0^{\delta}\left(\frac{\gamma}{\gamma-1}\frac{p_1}{\rho_s} + \frac{v_s^2}{2} - \frac{\gamma}{\gamma-1}\frac{p}{\rho} - \frac{u^2}{2}\right)\rho u\, dy$$

where p_1 is the static pressure at the edge of the boundary layer
p is the static pressure at a distance y from the surface
ρ_s is the density at the edge of the boundary layer
ρ is the density at a distance y from the surface
u is the velocity at a distance y from the surface
v_s is the velocity at the edge of the boundary layer
l is the length of slot.

Assuming that the pressure and density are constant throughout the boundary layer this may be written

$$\text{Energy lost per second} = \rho_s l v_s^3 \int_0^{\delta}\left[\tfrac{1}{2}\left\{1 - \left(\frac{u}{v_s}\right)^2\right\}\right]\frac{u}{v_s}\, dy$$

$$= \rho_s l v_s^3\, \vartheta s$$

where ϑ_s is the energy thickness of the boundary layer at the throat of the slot.

The loss in energy due to diffusion is assumed to be $f.\ \frac{1}{2}\rho_s v_s^2$ per unit volume so that the energy lost per second is given by

$$f\ .\ \tfrac{1}{2}\rho_s v_s^2(w - \delta_s^*)v_s\ .\ l$$

where δ_s^* is displacement thickness of the boundary layer at the slot throat.

The total energy lost per second is therefore

$$\rho_s l v_s^3 \vartheta_s + \tfrac{1}{2}\rho_s v_s^3 f \,.\, l(w - \delta_s^*)$$

and the power required to be supplied to the pump is

$$\frac{1}{\eta_p} \,.\, \rho_s v_s^3 l \left[\vartheta_s + \tfrac{1}{2} f w'\right]$$

where w' is the effective slot width $= w - \delta_s^*$

η_p is the efficiency of the pump.

If this power were required to overcome an extra profile drag, C_{Dp}, then the power required to be supplied to the power plant would be

$$\frac{1}{\eta_e} C_{Dp} \tfrac{1}{2}\rho_0 U_0^3 S$$

where η_e is the propulsive efficiency of the aircraft power plant.

The power required by the pump may therefore be regarded as due to an extra profile drag whose coefficient is given by

$$\frac{1}{\eta_p} \rho_s v_s^3 l \left[\vartheta_s + \tfrac{1}{2} f w'\right] = \frac{1}{\eta_e} C_{Dp} \tfrac{1}{2}\rho_0 U_0^3 S \,,$$

i.e., $$C_{Dp} = \frac{\eta_e}{\eta_p} \frac{\rho_s}{\rho_0} \frac{v_s^3}{U_0^3} \frac{lw}{S} \left[2\frac{\vartheta_s}{w} + f\frac{w'}{w}\right].$$

It is usual to assume that the two efficiencies are the same so that the expression becomes

$$C_{Dp} = \frac{\rho_s}{\rho_0}\left(\frac{v_s}{U_0}\right)^3 \frac{lw}{S}\left[2\frac{\vartheta_s}{w} + f\frac{w'}{w}\right]$$

$$= \left(\frac{C_Q}{F}\right)^3 \frac{\rho_s}{\rho_0} \cdot \frac{lw}{S} \cdot \left[2\frac{\vartheta_s}{w} + f\frac{w'}{w}\right]$$

where $$C_Q = \frac{\rho_s v_s l(w - \delta_s^*)}{\rho_0 U_0 S} = F \cdot \frac{v_s}{U_0} \cdot$$

TABLE 1

Model Data

Semi-span	56·25 in.
Mean chord	24·55 in.
Chord of parallel part of wing	25·00 in.
Aspect ratio	4·6
Half-wing area	9·59 sq ft
Sweepback angle of leading edge	40 deg
Spanwise extent of slot and porous leading edge, from body	50·00 in.
Maximum chordwise extent of porous leading edge	0 to 11·2 per cent
Chordwise position of suction slot	2·5 per cent
Mean width of suction slot (normal to leading edge)	0·18 per cent
Distance of pressure-plotting station from centre-line	37·50 in.
Spanwise extent of Fowler flap, from body	25·00 in.
Flap angle	40 deg
Flap chord	7·50 in.
Centre of leading-edge radius of flap below wing trailing edge	0·63 in.
Distance of mean quarter-chord point aft of nose of body	44·48 in.
Distance of assumed c.g. aft of nose of body	46·94 in.
Distance, from nose of body, of junction of wing leading edge with body	20·00 in.
Length of body	90·00 in.
Maximum diameter of body	12·00 in.

N.B.—All dimensions are measured parallel or normal to the body centre-line.

TABLE 2

Co-ordinates of Aerofoil Section (along wind)

(Modified HSA I *profile)*

x per cent chord	y per cent chord	x per cent chord	y per cent chord
0	0	57·822	4·560
0·616	1·013	65·451	4·020
2·447	2·082	72·700	3·341
5·450	2·788	79·389	2·607
9·549	3·431	85·355	1·907
14·645	3·989	90·451	1·291
20·611	4·445	94·550	0·796
27·301	4·780	97·553	0·430
34·549	4·980	99·384	0·176
42·178	5·028	100·000	0
50·000	4·903		

Leading-edge radius	= 1·4 per cent chord
Maximum thickness	=10·06 per cent chord
Maximum thickness occurs at	42·18 per cent chord

TABLE 3

Lift Coefficients Without Flap (Fig. 5)

Leading-edge slot $w = 0{\cdot}18$ per cent chord								11·2 per cent chord porous leading edge		7·5 per cent chord porous leading edge	
$R = 2{\cdot}58 \times 10^6$ $C_Q = 0{\cdot}00612$		$R = 2{\cdot}58 \times 10^6$ Slot filled in		$R = 1{\cdot}29 \times 10^6$ $C_Q = 0{\cdot}01194$		$R = 1{\cdot}29 \times 10^6$ Slot filled in		$R = 2{\cdot}58 \times 10^6$ $C_Q = 0{\cdot}00165$		$R = 1{\cdot}29 \times 10^6$ $C_Q = 0{\cdot}00307$	
α	C_L	α	C_L	α	C_L	α	C_L	α	C_L	α	C_L
0	−0·010	0	−0·020	0	−0·008	0	−0·022	+8·3	+0·500	+5·2	+0·305
+8·3	+0·490	+5·2	+0·282	5·2	+0·303	+5·2	+0·267	10·4	0·624	8·3	0·493
12·4	0·728	10·3	0·570	10·4	0·603	10·3	0·564	12·5	0·744	10·4	0·614
16·6	0·956	15·5	0·854	15·5	0·888	15·5	0·796	14·5	0·873	12·4	0·737
18·6	1·063	18·6	0·930	20·7	1·150	18·5	0·860	16·6	0·948	14·5	0·858
20·7	1·174	20·6	0·950	22·8	1·250	20·5	0·902	18·6	1·063	16·6	0·972
21·7	1·222	22·6	0·968	24·8	1·348	22·6	0·921	20·7	1·167	18·6	1·070
22·8	1·274	24·6	0·931	26·9	1·472	24·6	0·932	22·6	1·046	20·7	1·170
23·8	1·329			27·9	1·507					22·8	1·270
24·8	1·406			28·6	1·554					24·8	1·380
25·9	1·466			28·4	1·180					26·9	1·471
26·4	1·488									28·8	1·387
27·4	1·546										

TABLE 4

Lift Coefficients with Flap (Fig. 6)

Leading-edge slot $w = 0{\cdot}18$ per cent chord								11·2 per cent porous leading edge			
$R = 2{\cdot}58 \times 10^6$ $C_Q = 0{\cdot}00534$		$R = 2{\cdot}58 \times 10^6$ Ducts closed		$R = 1{\cdot}29 \times 10^6$ $C_Q = 0{\cdot}00929$		$R = 1{\cdot}29 \times 10^6$ Ducts closed		$R = 2{\cdot}58 \times 10^6$ $C_Q = 0{\cdot}00187$		$R = 1{\cdot}29 \times 10^6$ $C_Q = 0{\cdot}00437$	
α	C_L	α	C_L	α	C_L	α	C_L	α	C_L	α	C_L
0·3	0·555	0·3	0·526	0·3	0·524	0·3	0·508	10·8	1·245	16·9	1·521
5·6	0·920	5·5	0·894	10·7	1·136	5·5	0·794	12·8	1·368	19·0	1·617
10·8	1·252	10·7	1·200	21·0	1·699	10·7	1·094	14·9	1·480	21·0	1·745
12·8	1·364	12·8	1·305	23·0	1·800	12·7	1·151	16·9	1·586	23·1	1·824
14·9	1·484	14·8	1·336	25·1	1·911	14·7	1·176	18·0	1·634	25·2	1·956
15·9	1·541	16·8	1·325	25·8	1·312	16·7	1·214	18·9	1·440	26·8	1·350
16·8	1·587	18·8	1·307	26·1	1·956	18·7	1·230				
17·2	1·607					20·7	1·250				
17·8	1·304										

TABLE 5

Pitching-Moment Coefficients (Fig. 7)

Leading-edge slot $w = 0{\cdot}18$ per cent chord								2·5 per cent chord porous leading edge		11·2 per cent chord porous leading edge	
No flap				With flap				No flap		With flap	
$C_Q = 0{\cdot}0119$		Slot filled in		$C_Q = 0{\cdot}00929$		Ducts closed		$C_Q = 0{\cdot}00214$		$C_Q = 0{\cdot}00437$	
C_L	C_M	C_L	C_M	C_L	C_M	C_L	C_M	C_L	C_M	C_L	C_M
−0·008	+0·0053	−0·022	+0·0069	0·524	−0·1216	1·508	−0·1123	0·465	−0·0272	1·521	−0·2309
+0·303	−0·0123	+0·267	−0·0013	1·136	−0·1781	0·794	−0·1247	0·582	−0·0367	1·617	−0·2400
0·603	−0·0382	0·564	−0·0226	1·699	−0·2360	1·094	−0·1547	0·701	−0·0442	1·745	−0·2546
0·888	−0·0667	0·794	−0·0108	1·800	−0·2493	1·151	−0·1523	0·820	−0·0535	1·824	−0·2697
1·150	−0·0801	0·860	+0·0063	1·911	−0·2048	1·176	−0·1463	0·933	−0·0588	1·956	−0·2938
1·250	−0·0850	0·902	+0·0106	1·312	−0·1689	1·214	−0·1424	1·039	−0·0631	1·350	−0·2630
1·348	−0·1002	0·921	+0·0098			1·230	−0·1443	1·135	−0·0692		
1·472	−0·1223	0·932	−0·0028			1·250	−0·1646	1·256	−0·1002		
1·507	−0·1315							1·355	−0·1131		
1·554	−0·1425							1·420	−0·1198		
1·180	−0·0273							1·455	−0·1223		
								1·321	−0·1328		

TABLE 6

Lift/Drag Ratios (Fig. 8)

Leading-edge slot $w = 0{\cdot}18$ per cent chord										2·5 per cent chord porous leading edge				11·2 per cent chord porous leading edge			
$R = 2{\cdot}58 \times 10^6$				$R = 1{\cdot}29 \times 10^6$						$R = 1{\cdot}29 \times 10^6$		$R = 2{\cdot}58 \times 10^6$		$R = 1{\cdot}29 \times 10^6$			
No flap				No flap		No flap		With flap		No flap				With flap			
$C_Q = 0{\cdot}00612$		Slot filled in		$C_Q = 0{\cdot}01194$		Slot filled in		$C_Q = 0{\cdot}00929$		$C_Q = 0{\cdot}00214$		$C_Q = 0{\cdot}00093$		$C_Q = 0{\cdot}00437$		$C_Q = 0$	
C_L	C_D/C_L	C_L	C_D/C_L	C_L	C_D/C_L	C_L	C_D/C_L	C_L	C_D/C_L	C_L	C_D/C_L	C_L	C_D/C_L	C_L	C_D/C_L	C_L	C_D/C_L
																0·887	0·1498
																1·016	0·1770
+0·490	0·071	0·282	0·103	0·303	0·087	0·267	0·112	0·524	0·165	0·465	0·087	0·480	0·086	1·521	0·159	1·123	0·2105
0·728	0·079	0·570	0·097	0·603	0·084	0·564	0·137	1·136	0·145	0·582	0·088	0·600	0·107	1·617	0·161	1·178	0·2531
0·956	0·098	0·854	0·186	0·888	0·102	0·796	0·238	1·699	0·177	0·701	0·092	0·710	0·093	1·745	0·173	1·207	0·2970
1·063	0·113	0·930	0·270	1·150	0·124	0·860	0·297	1·800	0·187	0·820	0·101	1·820	0·101	1·824	0·191		
1·174	0·119	0·950	0·320	1·250	0·134	0·902	0·339	1·911	0·199	0·933	0·107	0·925	0·109	1·956	0·210		
1·222	0·123	0·968	0·371	1·348	0·146	0·921	0·390	1·956	0·205	1·039	0·125	1·027	0·119	1·350	0·461		
1·274	0·129	0·931	0·432	1·472	0·154	0·932	0·442	1·312	0·492	1·135	0·134	1·125	0·133				
1·329	0·134			1·507	0·173					1·256	0·164	1·110	0·261				
1·411	0·147			1·554	0·176					1·355	0·183						
1·466	0·155			1·180	0·436					1·420	0·214						
1·488	0·160									1·455	0·217						
1·546	0·168									1·321	0·346						

TABLE 7

Drag Coefficients (*Fig.* 9)

Leading-edge slot $w = 0{\cdot}18$ per cent chord								2·5 per cent chord porous leading edge			
$R = 2{\cdot}58 \times 10^6$				$R = 1{\cdot}29 \times 10^6$				$R = 2{\cdot}58 \times 10^6$		$R = 1{\cdot}29 \times 10^6$	
$C_Q = 0{\cdot}00612$		Slot filled in		$C_Q = 0{\cdot}01194$		Slot filled in		$C_Q = 0{\cdot}00093$		$C_Q = 0{\cdot}00214$	
C_L^2	C_D	C_L^2	C_D	C_L^2	C_D	C_L^2	C_D	C_L^2	C_D	C_L^2	C_D
0	0·0123	0	0·0207	0	0·0166	0	0·0201	0·230	0·0411	0·216	0·0405
0·240	0·0349	0·08	0·0291	0·092	0·0263	0·071	0·0298	0·360	0·0644	0·339	0·0511
0·530	0·0577	0·325	0·0535	0·364	0·0509	0·318	0·0773	0·504	0·0662	0·492	0·0645
0·914	0·0939	0·729	0·1586	0·788	0·0908	0·634	0·1892	0·673	0·0825	0·673	0·0826
1·130	0·1201	0·865	0·2511	1·323	0·1422	0·740	0·2553	0·857	0·1009	0·871	0·0998
1·378	0·1401	0·903	0·3035	1·563	0·1672	0·814	0·3053	1·054	0·1227	1·081	0·1247
1·623	0·1647										
1·991	0·2077	0·937	0·3590	1·817	0·1965	0·848	0·3593	1·266	0·1499	1·288	0·1519
2·149	0·2265	0·867	0·4017	2·167	0·2424	0·869	0·4123	1·232	0·2893	1·578	0·2053
2·214	0·2382			2·271	0·2601					1·836	0·2473
2·390	0·2592			2·415	0·2726					2·016	0·2942
				1·392	0·5154					2·117	0·3153
										1·715	0·4567

TABLE 8

Increments in $C_{L\max}$ with Flap (Figs. 10 and 11)

Leading-edge slot $w = 0{\cdot}18$ per cent chord									2·5 per cent chord porous leading edge					
$R = 2{\cdot}58 \times 10^6$			$R = 2{\cdot}24 \times 10^6$			$R = 1{\cdot}29 \times 10^6$			$R = 2{\cdot}58 \times 10^6$			$R = 1{\cdot}29 \times 10^6$		
$\Delta C_{L\max}$	C_Q	C_{Dp}	$\Delta C_{L\max}$	C_Q	C_{Dp}	$\Delta C_{L\max}$	C_Q	C_{Dp}	$\Delta C_{L\max}$	C_Q	C_{Dp}	$\Delta C_{L\max}$	C_Q	C_{Dp}
0·01	0·0042	0·0216	0·13	0·0044	0·0275	0·05	0·0034	0·0124	0·09	0·0006	0·0018	0·01	0·0012	0·0229
0·10	0·0047	0·0274	0·30	0·0054	0·0417	0·10	0·0055	0·0382	0·16	0·0009	0·0096	0·28	0·0018	0·0703
0·23	0·0050	0·0335	0·52	0·0066	0·0633	0·45	0·0068	0·0650	0·21	0·0011	0·0142	0·47	0·0022	0·1222
0·29	0·0054	0·0393	0·65	0·0067	0·0841	0·68	0·0080	0·1191	0·23	0·0012	0·0263	0·54	0·0026	0·2386
0·44	0·0059	0·0473	0·68	0·0071	0·1116	0·77	0·0091	0·1538	0·25	0·0013	0·0347	0·56	0·0025	0·1919
						0·80	0·0104	0·2224						
						0·81	0·0109	0·2754						

Values of $C_{L\max}$ Without Suction

$R \times 10^{-6}$	$C_{L\max}$
1·29	1·24
2·24	1·31
2·58	1·35

TABLE 9

Increments in $C_{L\max}$ Without Flap (Figs. 10 and 12)

Leading-edge slot									2·5 per cent chord porous leading edge						11·2 per cent chord porous leading edge		
$w = 0{\cdot}18$ per cent chord						$w = 0{\cdot}44$ per cent chord			$R = 2{\cdot}58 \times 10^6$			$R = 1{\cdot}29 \times 10^6$			$R = 1{\cdot}29 \times 10^6$		
$R = 2{\cdot}5 \times 10^6$			$R = 1{\cdot}29 \times 10^6$			$R = 1{\cdot}29 \times 10^6$											
$\Delta C_{L\max}$	C_Q	C_{Dp}	$\Delta C_{L\max}$	C_Q	C_{Dp}	$\Delta C_{L\max}$	C_Q	C_{Dp}	$\Delta C_{L\max}$	C_Q	C_{Dp}	$\Delta C_{L\max}$	C_Q	C_{Dp}	$\Delta C_{L\max}$	C_Q	C_{Dp}
												−0·02	0·0012	0·0218			
0·10	0·0041	0·0223	0·03	0·0033	0·0155	0·20	0·0086	0·085	0·02	0·0005	0·0020	0	0·0015	0·0425	−0·01	0·0016	
0·24	0·0050	0·0362	0·144	0·0065	0·0617	0·28	0·0099	0·098	0·10	0·0008	0·0070	0·31	0·0021	0·1084	0·09	0·0023	
0·41	0·0053	0·0535	0·35	0·0068	0·0660	0·41	0·0105	0·122	0·14	0·0009	0·0108	0·32	0·0021	0·1133	0·26	0·0031	
0·51	0·0056	0·0670	0·43	0·0071	0·0761	0·52	0·0115	0·132	0·19	0·0013	0·0287	0·43	0·0026	0·2142	0·42	0·0036	
0·55	0·0058	0·0794	0·48	0·0074	0·0832	0·65	0·0135	0·167	0·23	0·0014	0·0372	0·45	0·0027	0·2936	0·57	0·0044	
0·61	0·0061	0·1129	0·55	0·0077	0·1033				0·24	0·0013	0·0390	0·46	0·0027	0·2937	0·60	0·0052	
			0·58	0·0089	0·1522							0·49	0·0027	0·2609	0·64	0·0054	
			0·62	0·0103	0·2606												
			0·63	0·0113	0·3803												
			0·64	0·0119	0·5002												
			0·64	0·0123	0·7463												

Values of $C_{L\max}$ Without Suction

$R \times 10^{-6}$	$C_{L\max}$
1·29	0·93
2·58	0·94

TABLE 10

Pressure Distributions (*Figs.* 13, 14 *and* 15)

$$C_p = \frac{p - p_0}{\frac{1}{2}\rho_0 U_0^2}$$

	Leading-edge slot $w=0{\cdot}18$ per cent chord						11·2 per cent chord porous leading edge						2·5 per cent chord porous leading edge	
α C_L R C_Q	Before stall No flap 25·9 deg 1·45 1·29 × 10⁶ 0·00763		Before stall With flap 26·0 deg 1·93 1·29 × 10⁶ 0·00768		Before stall No flap 10·4 deg 0·60 1·29 × 10⁶ 0·0125		Before stall With flap 26·0 deg 1·93 1·29 × 10⁶ 0·00407		After stall With flap 26·0 deg 1·40 1·29 × 10⁶ 0·00424		Before stall No flap 10·4 deg 0·60 1·29 × 10⁶ 0·0019		Before stall No flap 25·9 deg 1·42 1·29 × 10⁶ 0·0020	
x/c	U.S.	L.S.	U.S.	L.S.	U.S.	L.S.	U.S.	L.S.	U.S.	L.S.	U.S.	L.S.	U.S.	L.S.
0	−14·552		−19·914		−2·204		−17·940		−3·555		−1·792		−12·653	
0·004	−16·653	—	−21·95	—	−4·334	—	—	—	—	—	—	—	—	—
0·013	−15·515	−3·455	−20·096	−5·651	−5·401	+0·463	−15·831	−4·479	−2·210	−0·743	−3·680	+0·583	−11·654	−2·966
0·021	−11·373	—	−14·324	—	−6·104	—	—	—	—	—	—	—	—	—
0·025	—	−0·602	—	−2·219	—	+0·570	−8·738	−1·536	−1·646	+0·119	−2·310	+0·591	−6·511	−0·622
0·032	−3·995	—	−5·261	—	−0·309	—	—	—	—	—	—	—	—	—
0·050	−3·871	+0·234	−5·105	−0·187	−1·111	+0·541	−4·698	−0·097	−1·168	+0·447	−1·445	+0·529	−4·129	+0·275
0·100	−2·284	+0·603	−3·117	+0·459	−0·931	+0·397	−3·374	+0·440	−1·128	+0·547	−1·108	+0·397	−2·323	+0·621
0·15	−1·736	+0·646	−2·349	+0·604	−0·777	+0·309	−2·307	+0·554	−1·003	+0·525	−0·819	+0·335	−1·598	+0·649
0·20	−1·415	+0·628	−1·923	+0·615	−0·681	+0·246	−1·928	+0·569	−0·819	+0·508	−0·747	+0·242	−1·186	+0·624
0·30	−0·901	+0·533	−1·348	+0·570	−0·501	+0·140	−1·388	+0·453	−0·873	+0·372	−0·563	+0·141	−0·813	+0·521
0·40	−0·598	+0·442	−1·025	+0·496	−0·460	+0·081	−1·046	+0·458	−0·855	+0·307	−0·470	+0·079	−0·708	+0·424
0·50	−0·313	+0·351	−0·728	+0·418	−0·368	+0·029	−0·865	+0·390	−0·810	+0·213	−0·387	+0·024	−0·636	+0·325
0·60	−0·182	+0·260	−0·457	+0·333	−0·269	−0·008	−0·701	+0·305	−0·739	+0·097	−0·289	−0·003	−0·572	+0·223
0·70	−0·171	+0·194	−0·272	+0·236	−0·172	−0·004	−0·532	+0·241	−0·694	−0·019	−0·184	−0·015	0·532	+0·155
0·80	−0·189	+0·143	−0·224	+0·199	−0·063	+0·25	−0·375	+0·189	−0·684	−0·070	−0·074	−0·024	−0·518	+0·088
0·90	−0·226	+0·059	−0·272	+0·103	+0·052	+0·062	−0·333	+0·114	−0·637	−0·189	+0·039	−0·053	−0·512	−0·004
0·95	−0·226	−0·014	−0·309	+0·032	+0·092	+0·110	−0·303	+0·054	−0·618	−0·289	+0·077	−0·066	−0·398	−0·094
1·00	−0·167		−0·172		+0·128		−0·139		−0·563		+0·125		−0·283	

U.S. signifies Upper Surface
L.S. signifies Lower Surface

TABLE 11

Sink Effect Near Slot (*Figs.* 17 *and* 18)

$$C_p = \frac{p - p_0}{\frac{1}{2}\rho_0 U_0^2}$$

α C_Q	10·4 deg 0·0037	10·4 deg 0·0081	25·9 deg 0·01206
s/c	C_p	C_p	C_p
0	−1·884	−2·054	−14·552
0·0115	−3·706	−3·981	−16·653
0·0220	−4·348	−4·840	−15·515
0·0310	−4·043	−4·990	−11·373
0·0422	−1·418	−0·860	− 3·995
0·0612	−1·391	−1·228	− 3·871
0·1122	−1·014	−0·945	− 2·284

Other values tabulated in Table 10.

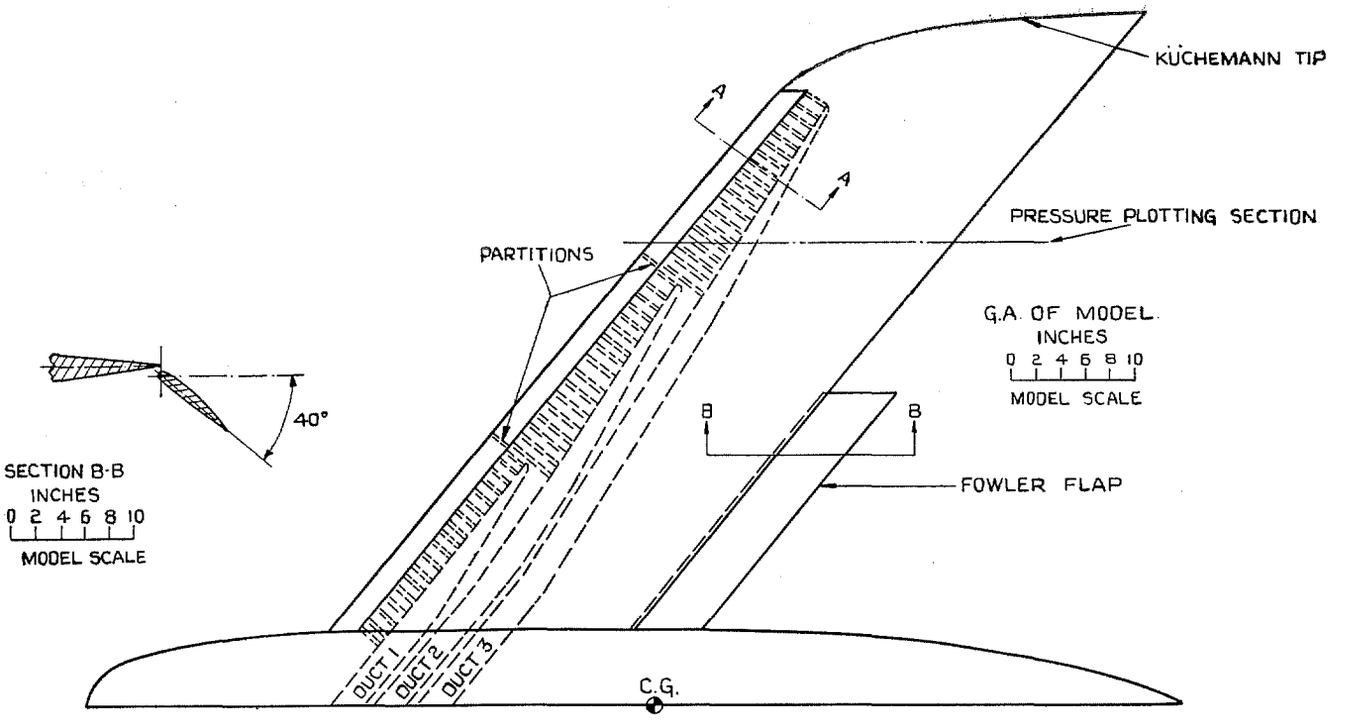

FIG. 1. Sketch of Model.

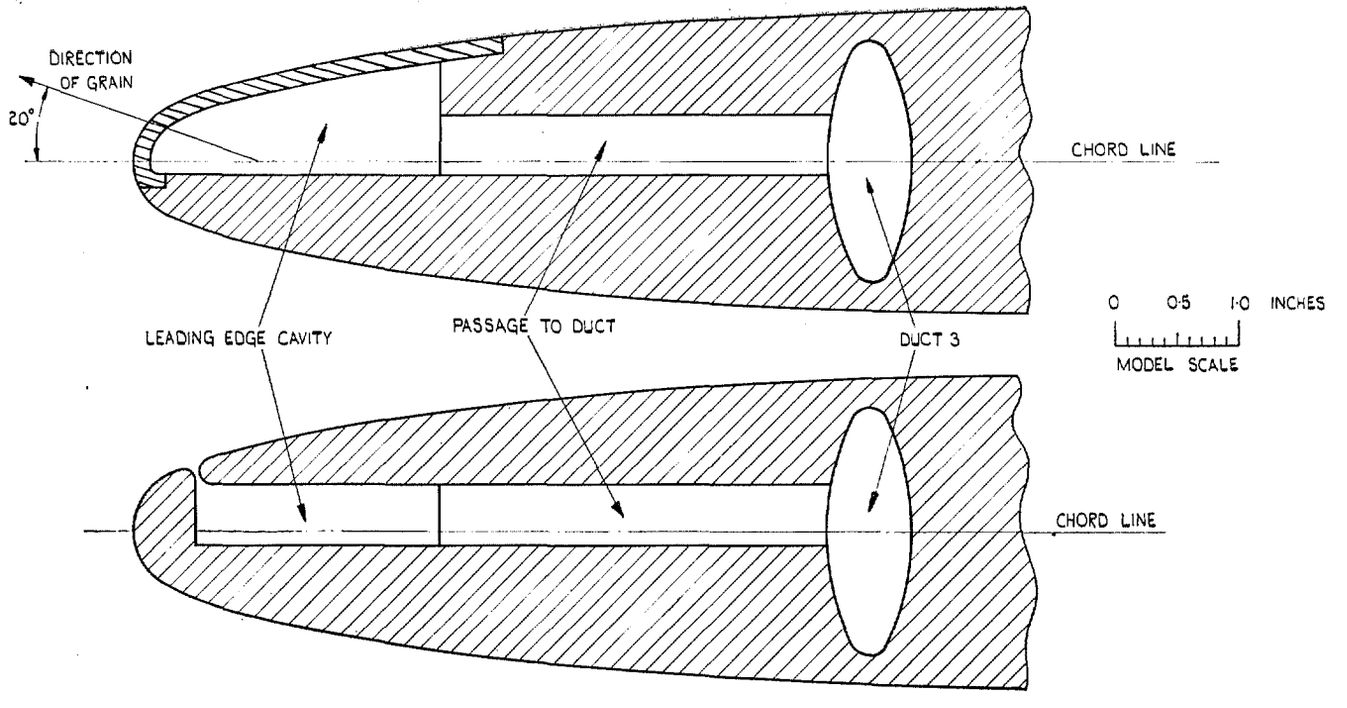

FIG. 2. Detail of leading edge of model (section A—A).

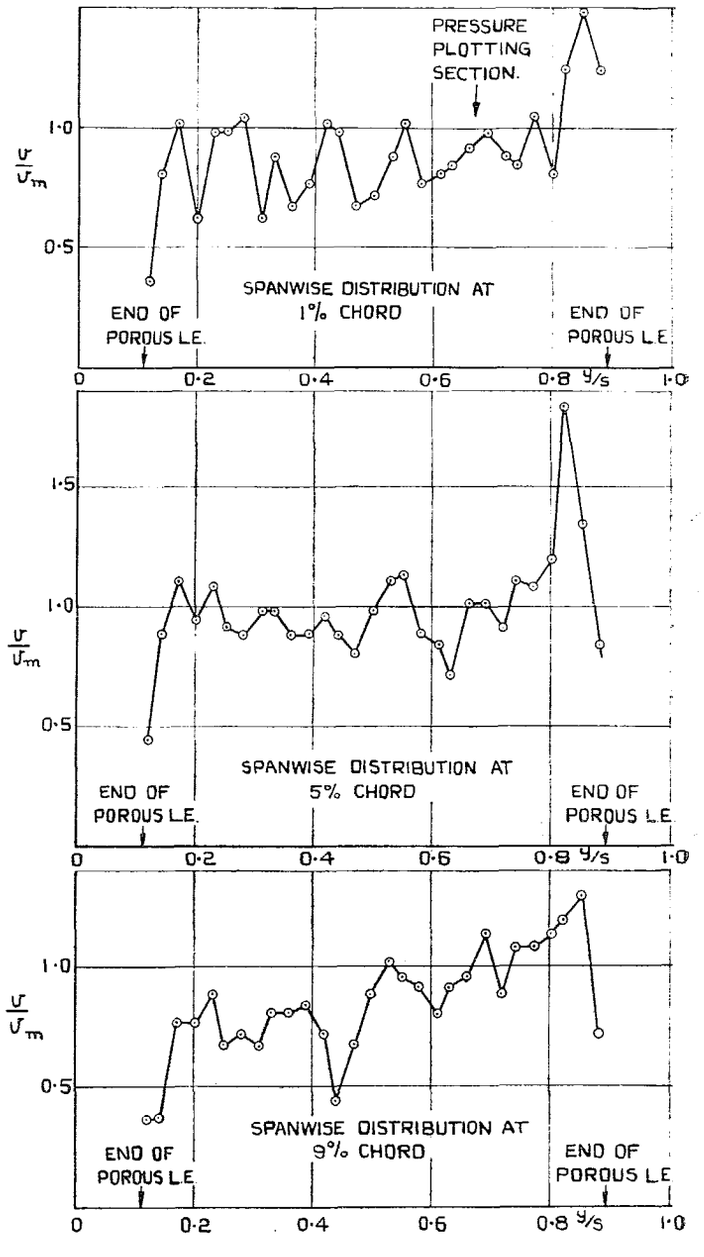

FIG. 3. Distribution of flow into porous leading edge.

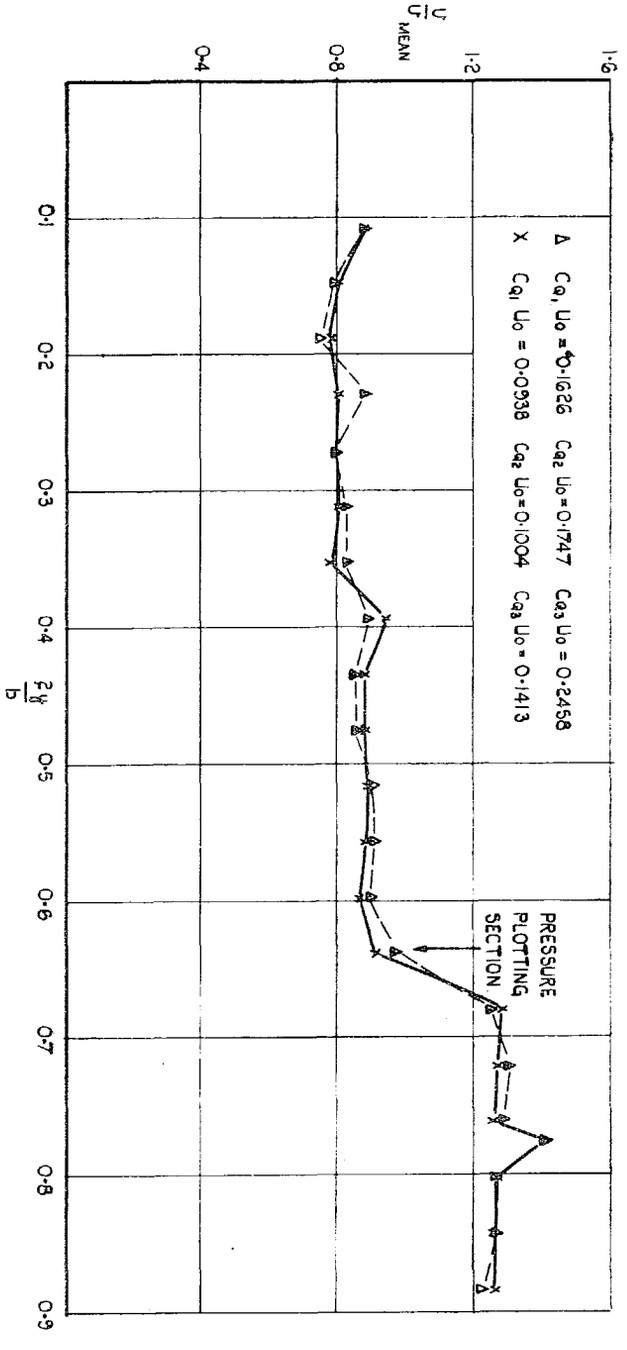

FIG. 4. Distribution of slot velocity.

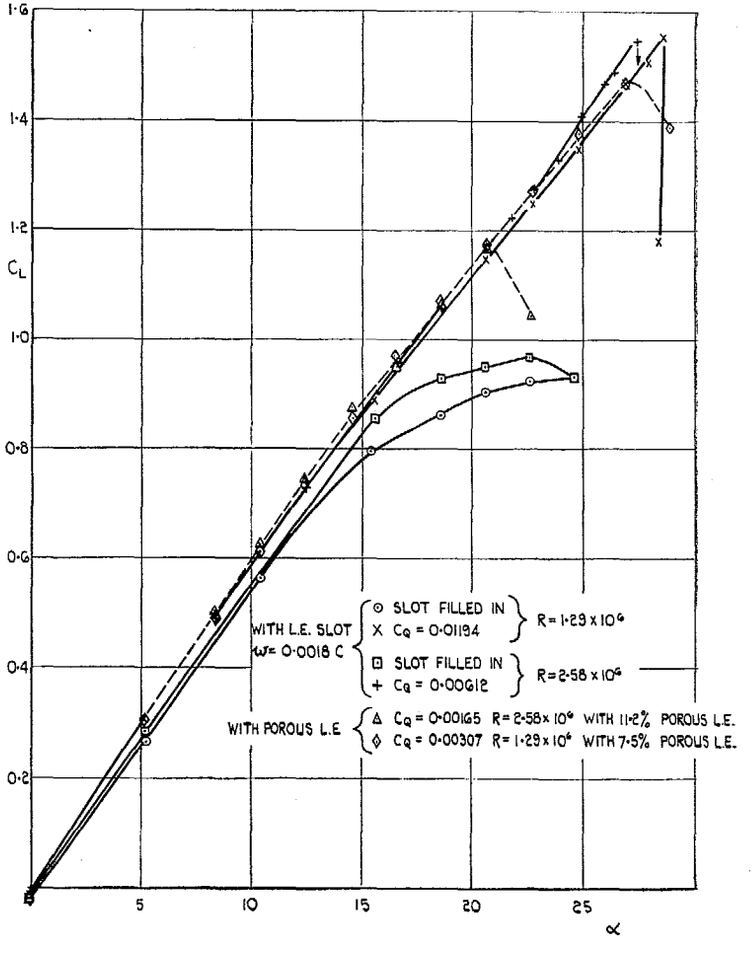

FIG. 5. Lift coefficients without flap.

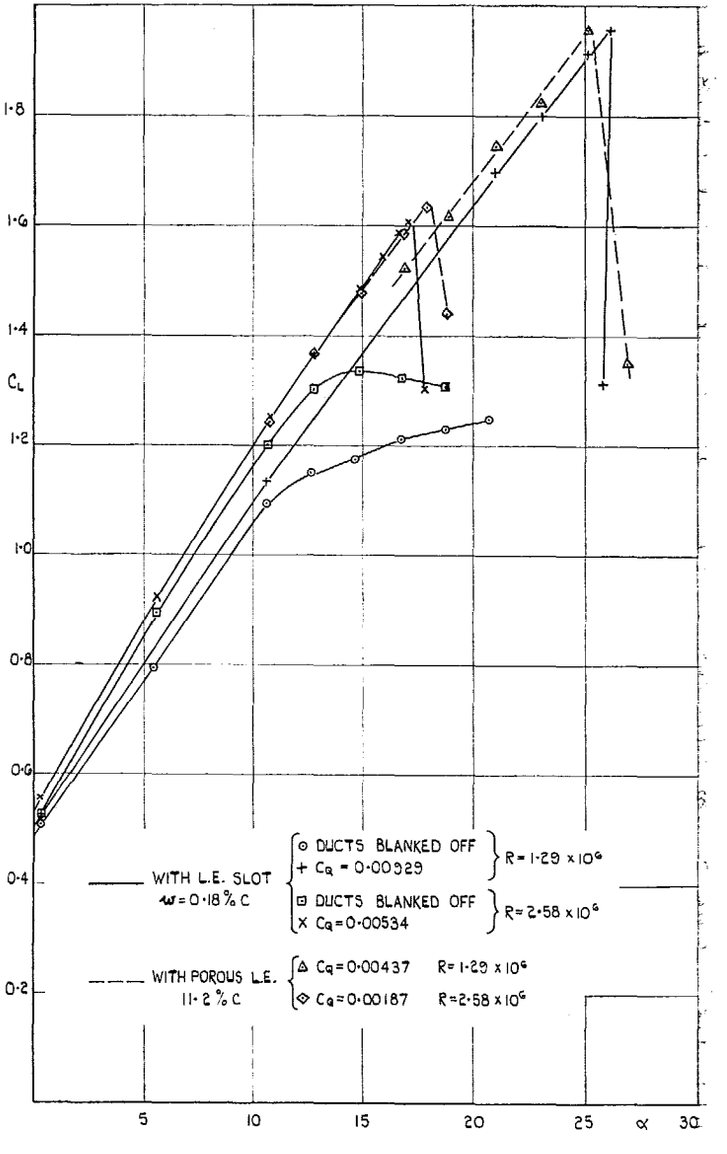

FIG. 6. Lift coefficients with flap.

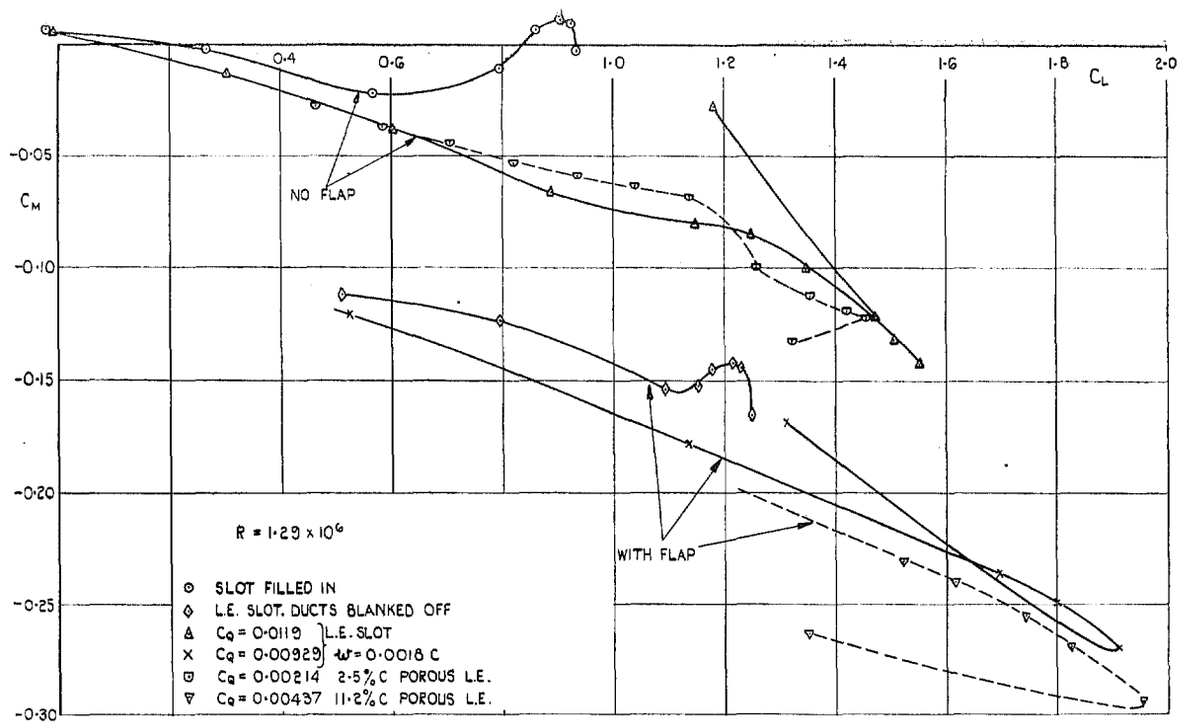

FIG. 7. Pitching-moment coefficients.

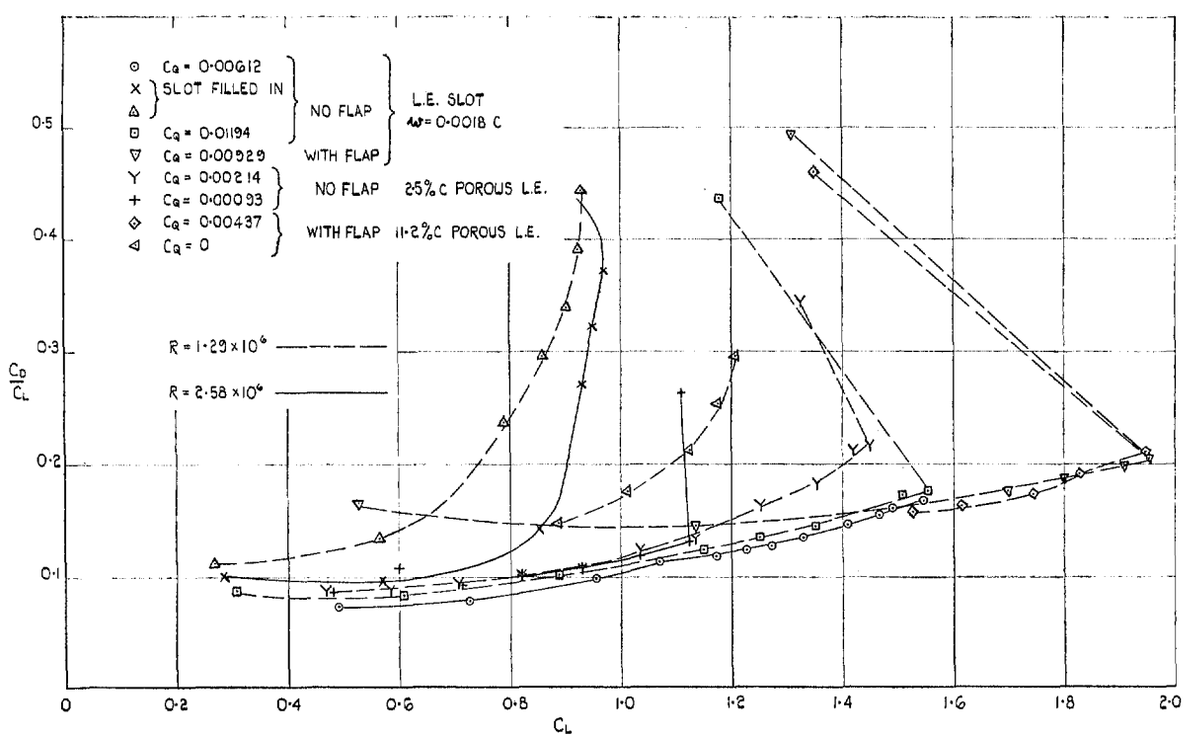

FIG. 8. Lift/drag ratios.

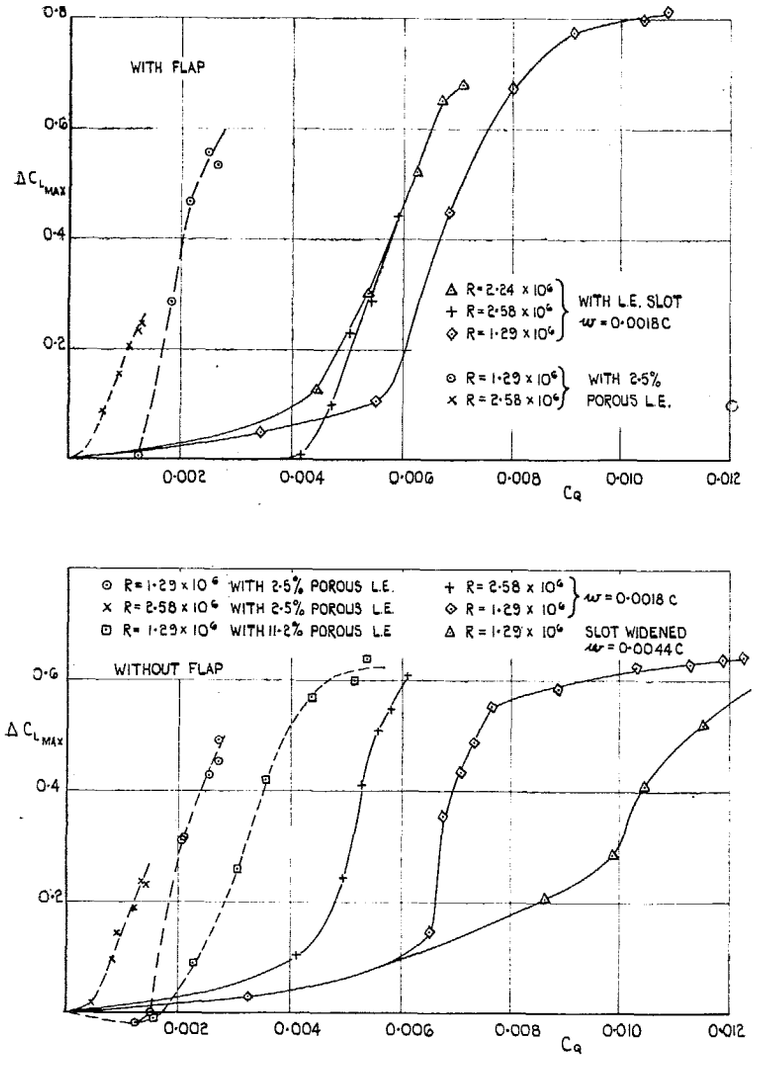

FIG. 10. Increments in $C_{L\,max}$.

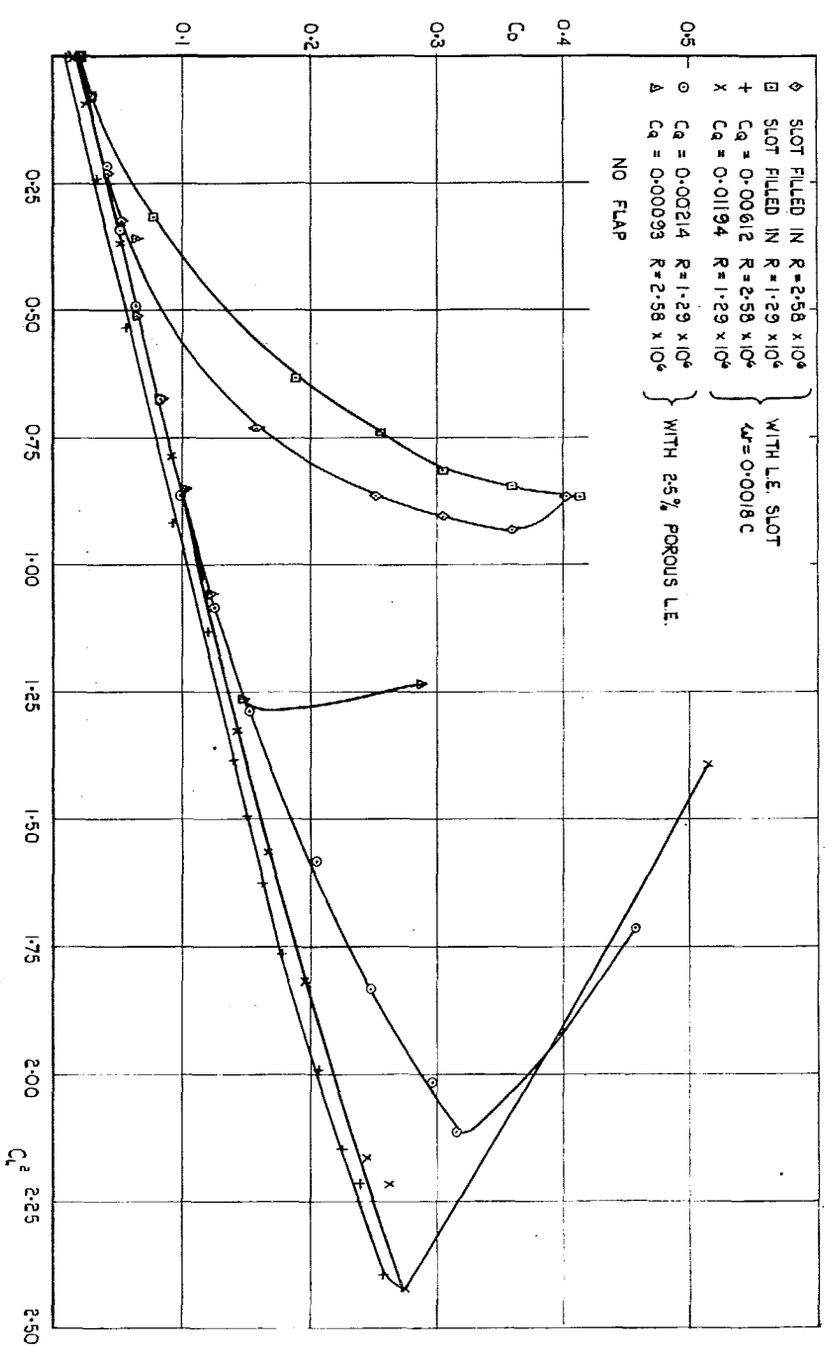

FIG. 9. Drag coefficients.

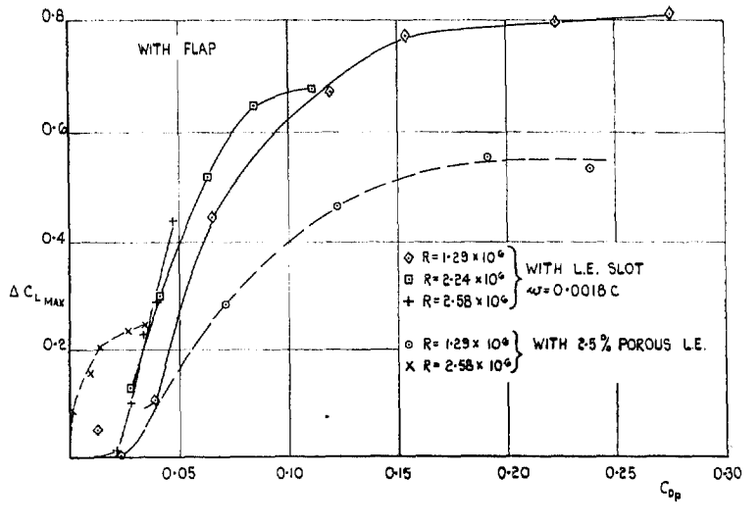

FIG. 11. Pump drag coefficients.

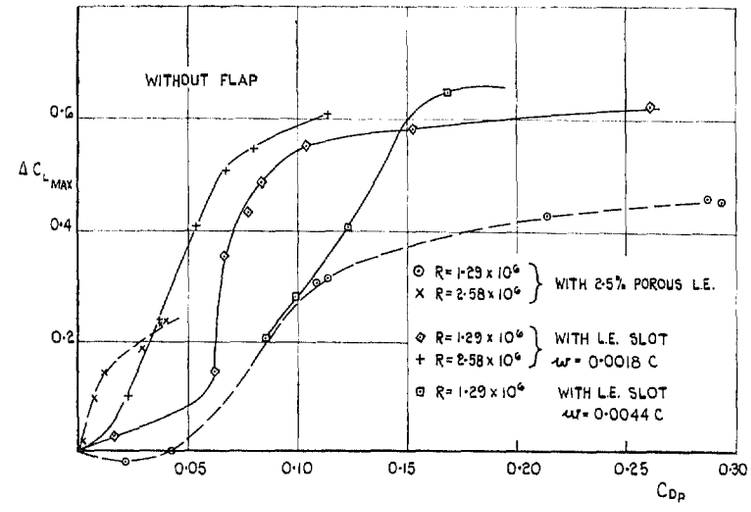

FIG. 12. Pump drag coefficients.

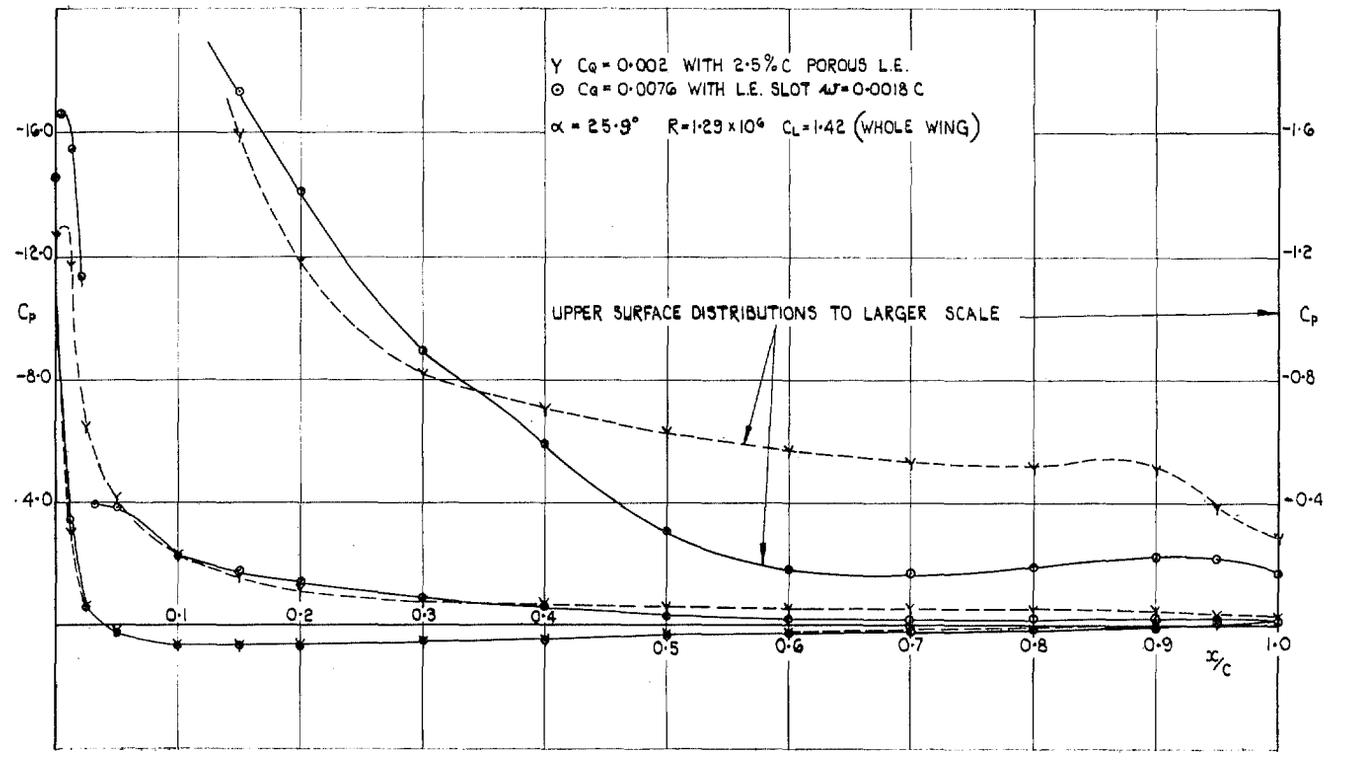

FIG. 13. Chordwise pressure distribution without flap.

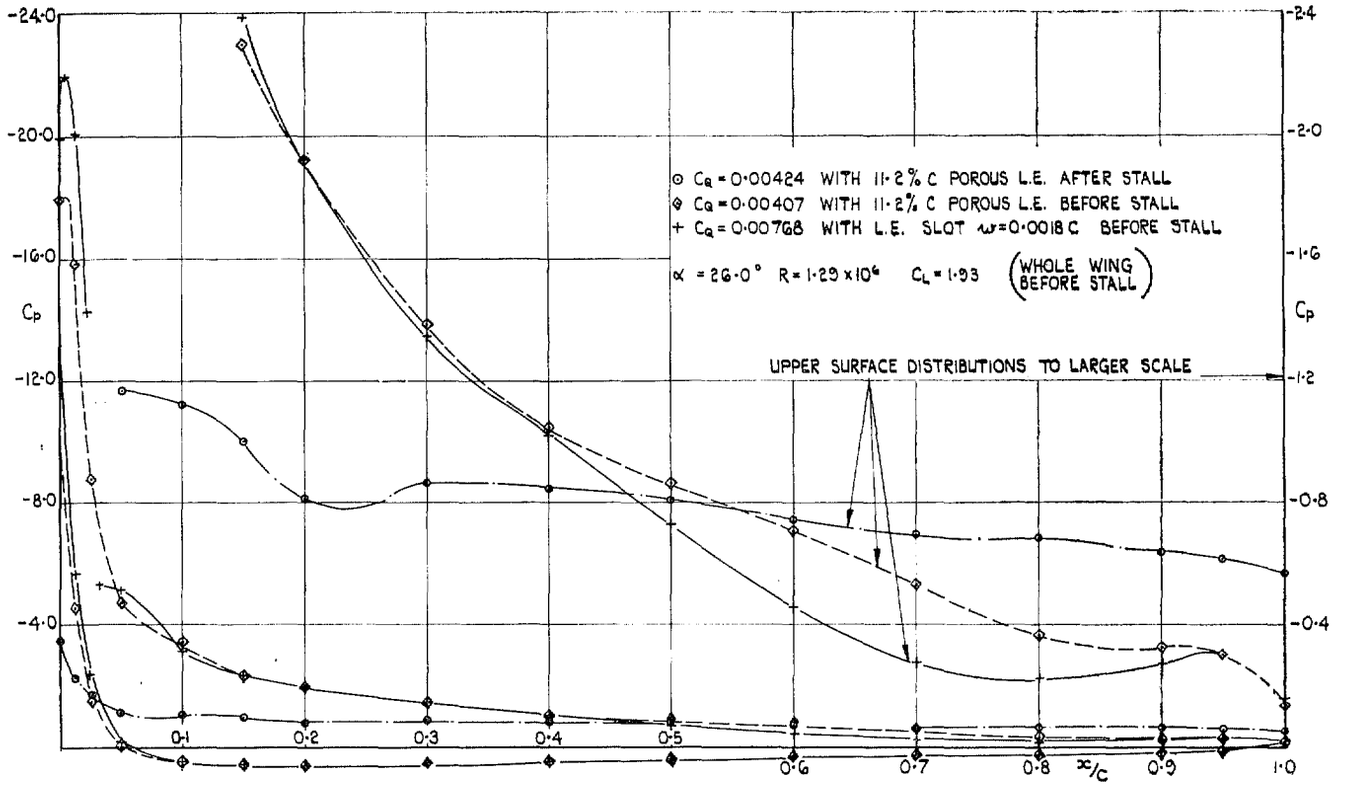

FIG. 14. Chordwise pressure distribution with flap.

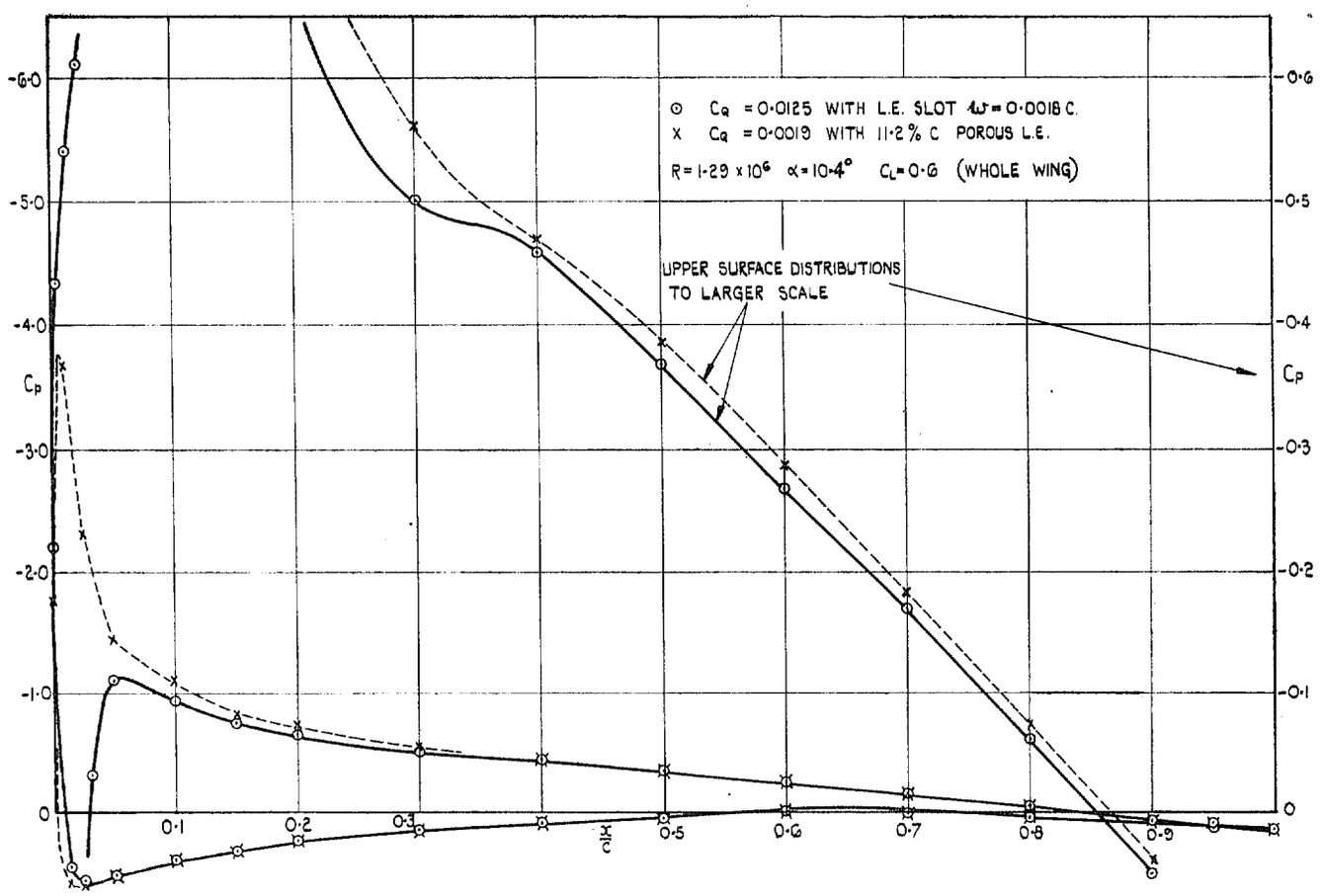

FIG. 15. Chordwise pressure distribution without flap.

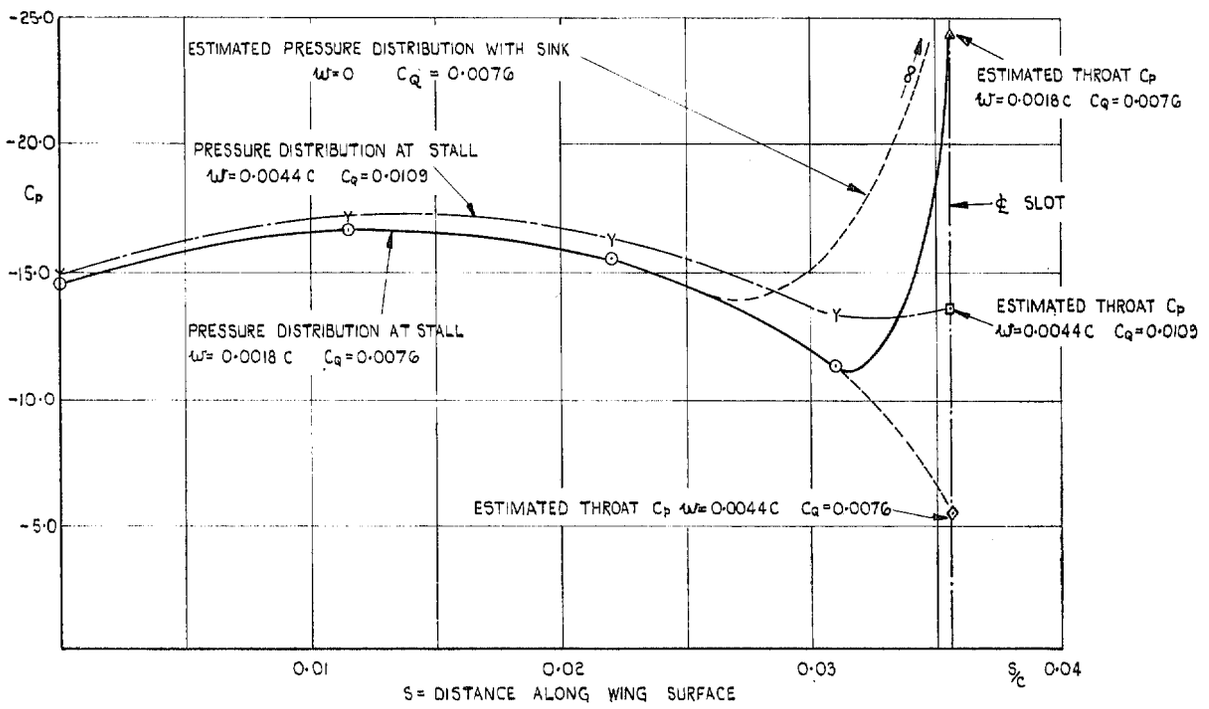

FIG. 16. Pressure distribution near the slot. $\alpha = 25 \cdot 9$ deg.

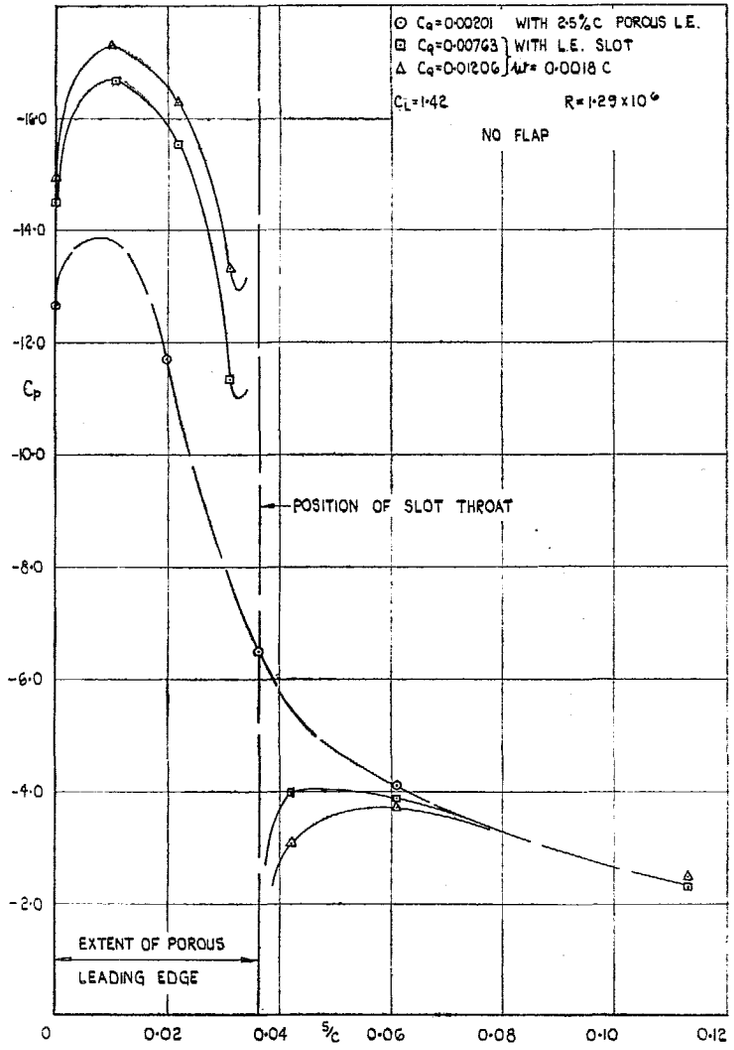

FIG. 17. Sink effect near slot. $\alpha = 25{\cdot}9$ deg.

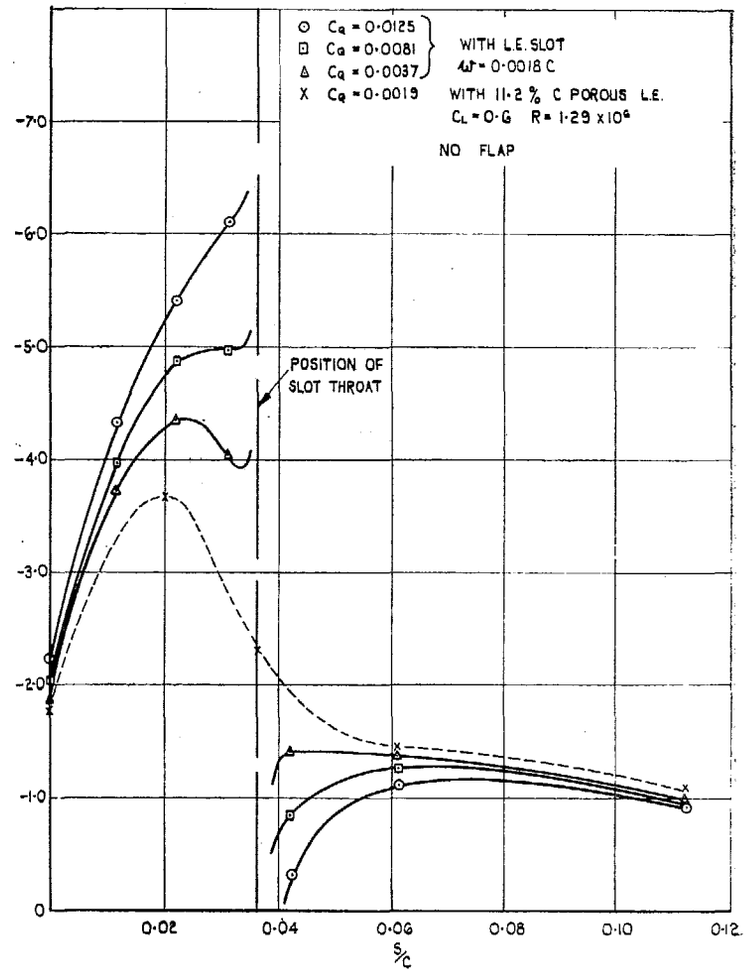

FIG. 18. Sink effect near slot. $\alpha = 10{\cdot}4$ deg.

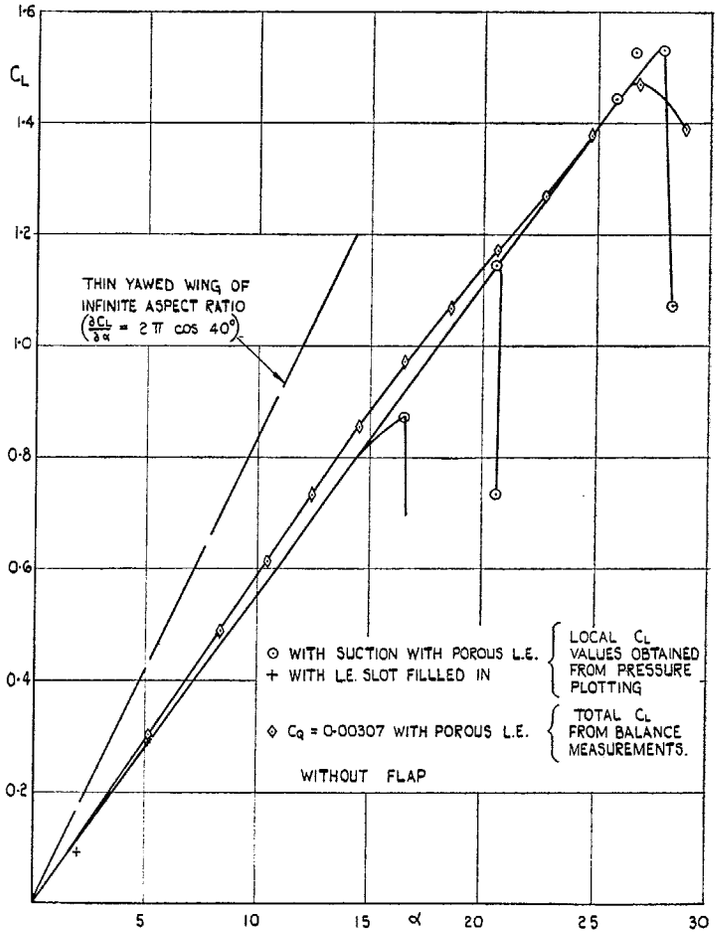

FIG. 19. Local lift coefficients.

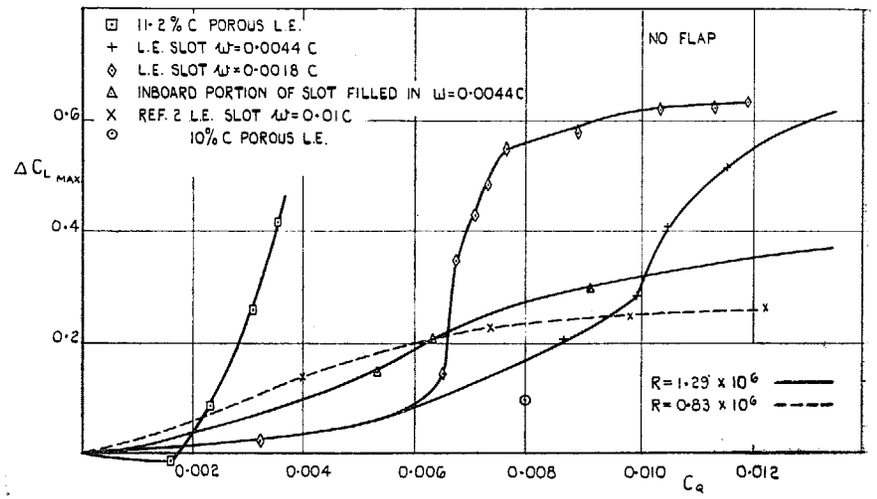

FIG. 20. Increments in $C_{L\,\max}$. Comparison with other tests.

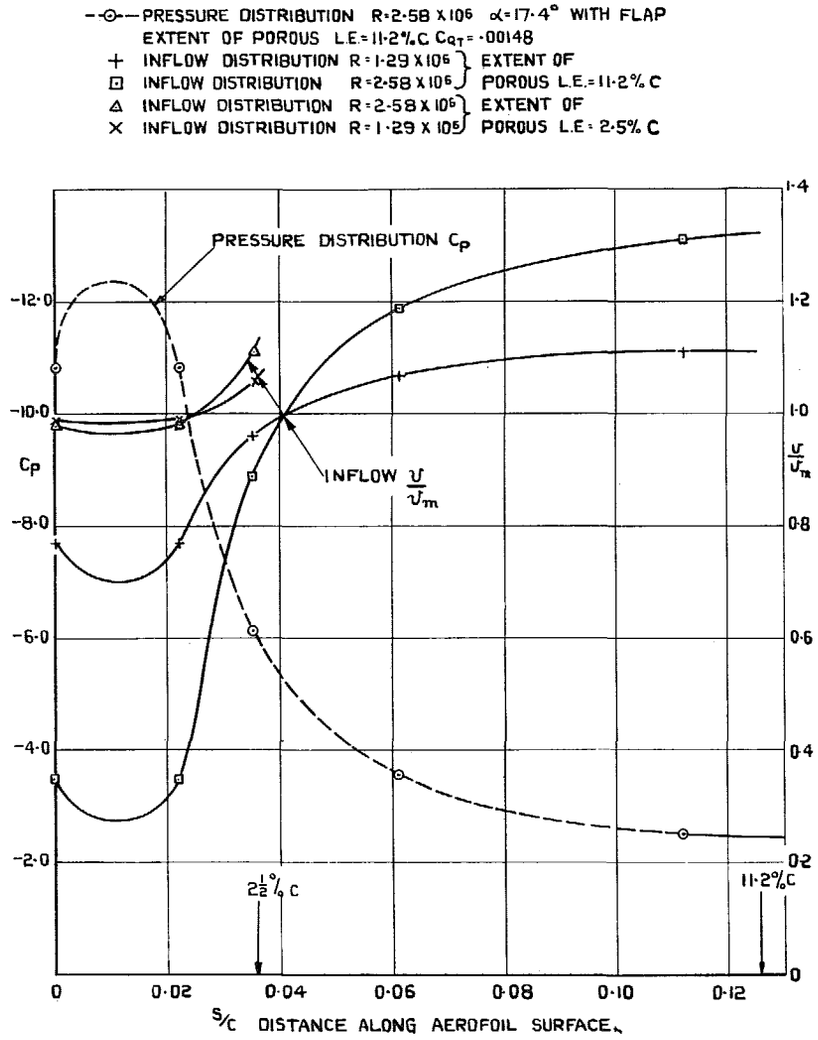

FIG. 22. Pressure distribution with corresponding flow into porous leading edge.

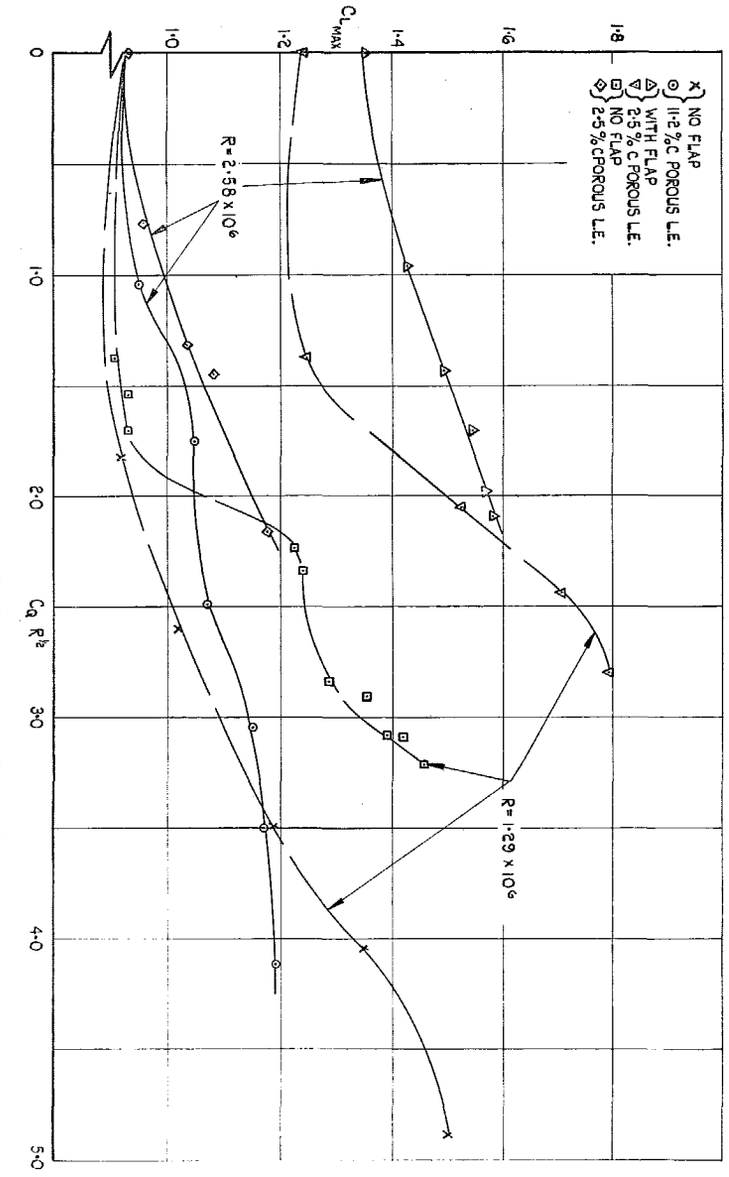

FIG. 21. Scale effect on C_q for porous leading edge.

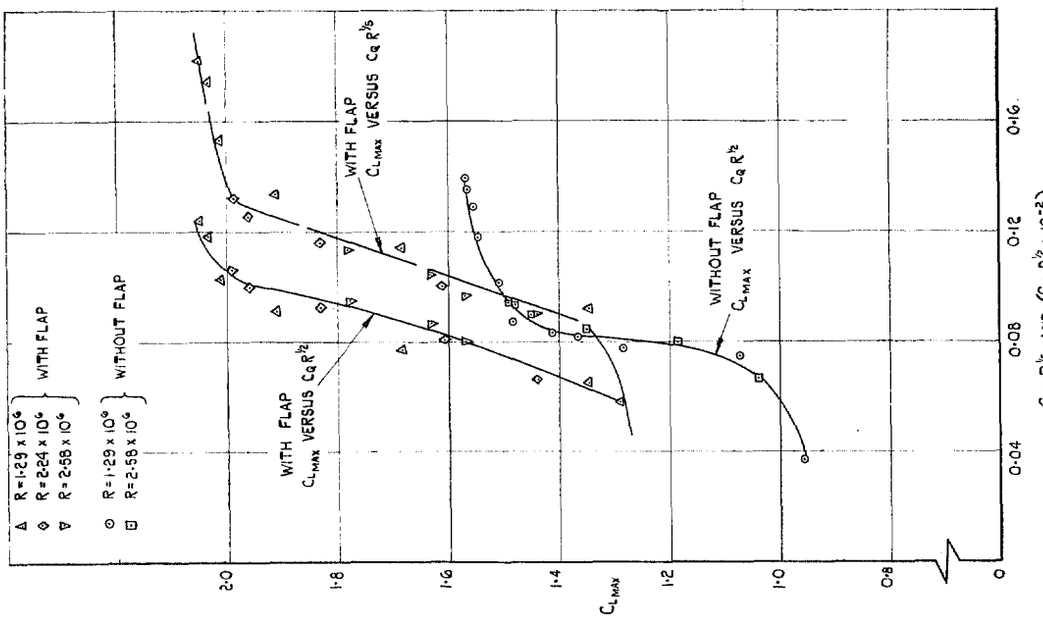

FIG. 23. Scale effect on C_q for slot.

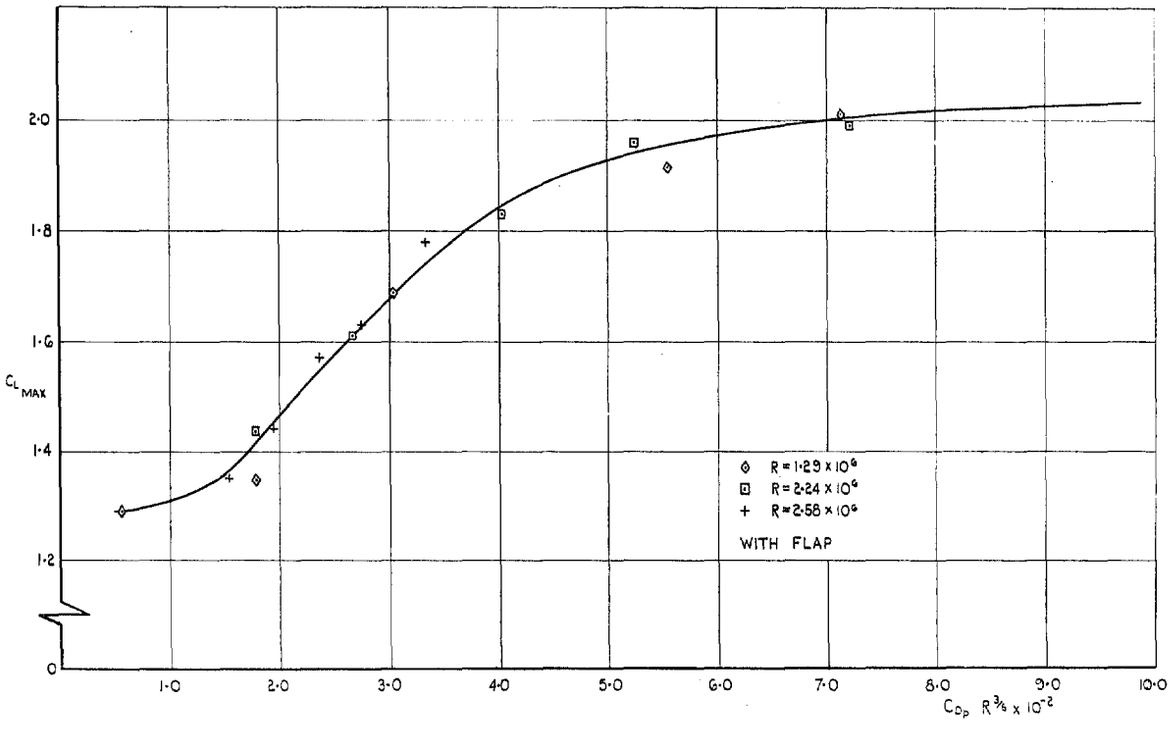

FIG. 24. Scale effect on C_{Dp} for slot.

J4313 Wt.18/9296 K9 2/55 D&Co. 34/263

PRINTED IN GREAT BRITAIN

Publications of the Aeronautical Research Council

ANNUAL TECHNICAL REPORTS OF THE AERONAUTICAL RESEARCH COUNCIL (BOUND VOLUMES)

1936 Vol. I. Aerodynamics General, Performance, Airscrews, Flutter and Spinning. 40*s*. (41*s*. 1*d*).

Vol. II. Stability and Control, Structures, Seaplanes, Engines, etc. 50*s*. (51*s*. 1*d*.)

1937 Vol. I. Aerodynamics General, Performance, Airscrews, Flutter and Spinning. 40*s*. (41*s*. 1*d*.)

Vol. II. Stability and Control, Structures, Seaplanes, Engines, etc. 60*s*. (61*s*. 1*d*.)

1938 Vol. I. Aerodynamics General, Performance, Airscrews. 50*s*. (51*s*. 1*d*.)

Vol. II. Stability and Control, Flutter, Structures, Seaplanes, Wind Tunnels, Materials. 30*s*. (31*s*. 1*d*.)

1939 Vol. I. Aerodynamics General, Performance, Airscrews, Engines. 50*s*. (51*s*. 1*d*.)

Vol. II. Stability and Control, Flutter and Vibration, Instruments, Structures, Seaplanes, etc. 63*s*. (64*s*. 2*d*.)

1940 Aero and Hydrodynamics, Aerofoils, Airscrews, Engines, Flutter, Icing, Stability and Control, Structures, and a miscellaneous section. 50*s*. (51*s*. 1*d*.)

1941 Aero and Hydrodynamics, Aerofoils, Airscrews, Engines, Flutter, Stability and Control, Structures. 63*s*. (64*s*. 2*d*.)

1942 Vol. I. Aero and Hydrodynamics, Aerofoils, Airscrews, Engines. 75*s*. (76*s*. 3*d*.)

Vol. II. Noise, Parachutes, Stability and Control, Structures, Vibration, Wind Tunnels. 47*s*. 6*d*. (48*s*. 7*d*.)

1943 Vol. I. Aerodynamics, Aerofoils, Airscrews, 80*s*. (81*s*. 4*d*.)

Vol. II. Engines, Flutter, Materials, Parachutes, Performance, Stability and Control, Structures. 90*s*. (91*s*. 6*d*.)

1944 Vol. I. Aero and Hydrodynamics, Aerofoils, Aircraft, Airscrews, Controls. 84*s*. (85*s*. 8*d*.)

Vol. II. Flutter and Vibration, Materials, Miscellaneous, Navigation, Parachutes, Performance, Plates, and Panels, Stability, Structures, Test Equipment, Wind Tunnels. 84*s*. (85*s*. 8*d*.)

ANNUAL REPORTS OF THE AERONAUTICAL RESEARCH COUNCIL—

1933–34	1*s*. 6*d*. (1*s*. 8*d*.)	1937	2*s*. (2*s*. 2*d*.)
1934–35	1*s*. 6*d*. (1*s*. 8*d*.)	1938	1*s*. 6*d*. (1*s*. 8*d*.)
April 1, 1935 to Dec. 31, 1936.	4*s*. (4*s*. 4*d*.)	1939–48	3*s*. (3*s*. 2*d*.)

INDEX TO ALL REPORTS AND MEMORANDA PUBLISHED IN THE ANNUAL TECHNICAL REPORTS, AND SEPARATELY—

April, 1950 - - - - R. & M. No. 2600. 2*s*. 6*d*. (2*s*. 7½*d*.)

AUTHOR INDEX TO ALL REPORTS AND MEMORANDA OF THE AERONAUTICAL RESEARCH COUNCIL—

1909–1949 - - - - - R. & M. No. 2570. 15*s*. (15*s*. 3*d*.)

INDEXES TO THE TECHNICAL REPORTS OF THE AERONAUTICAL RESEARCH COUNCIL—

December 1, 1936 — June 30, 1939.	R. & M. No. 1850.	1*s*. 3*d*. (1*s*. 4½*d*.)
July 1, 1939 — June 30, 1945.	R. & M. No. 1950.	1*s*. (1*s*. 1½*d*.)
July 1, 1945 — June 30, 1946.	R. & M. No. 2050.	1*s*. (1*s*. 1½*d*.)
July 1, 1946 — December 31, 1946.	R. & M. No. 2150.	1*s*. 3*d*. (1*s*. 4½*d*.)
January 1, 1947 — June 30, 1947.	R. & M. No. 2250.	1*s*. 3*d*. (1*s*. 4½*d*.)
July, 1951 - - - -	R. & M. No. 2350.	1*s*. 9*d*. (1*s*. 10½*d*.)

Prices in brackets include postage.

Obtainable from

HER MAJESTY'S STATIONERY OFFICE

York House, Kingsway, London W.C 2 ; 423 Oxford Street, London W 1 (Post Orders : P O. Box No. 569, London S.E.1) ; 13A Castle Street, Edinburgh 2 ; 39 King Street, Manchester 2 ; 2 Edmund Street, Birmingham 3 ; 109 St Mary Street, Cardiff ; Tower Lane, Bristol 1 , 80 Chichester Street, Belfast OR THROUGH ANY BOOKSELLER

S.O. Code No. 23-2897